Triple oxygen isotope systematics as a tracer of fluids in the crust: A study from modern geothermal systems of Iceland

Zakharov D.O.[1], Bindeman I.N.[1], Tanaka R.[2], Friðleifsson G.Ó.[3], Reed M.[1] and Hampton, R.L.[1]

1- Department of Earth Sciences, 1272 University of Oregon, Eugene, OR, 97403 USA

2- The Pheasant Memorial Laboratory for Geochemistry and Cosmochemistry, Institute for Planetary Materials, Okayama University, Misasa, 682-0193, Japan

3- HS Orka, Svartsengi, 240 Grindavik, Iceland

Revised submission to Chemical Geology (CHEMGE12287)

Abstract: 416 words

Main text with figures, figure captions and formulas: 8400 words

9 figures and 1 table

ABSTRACT

Mass-dependent fractionation of triple oxygen isotopes during water-rocks interaction has been previously used to constrain environmental conditions of the Precambrian. To validate those studies, we report high-precision triple oxygen isotope measurements (expressed as $\Delta'_{17}O$ with reference slope 0.528) of quartz, epidote and well fluids from Krafla and Reykjanes geothermal areas of Iceland as well as measurements from the extinct 6 Ma Geitafell hydrothermal system. At these systems, basalts reacted with distinct fluid sources at temperatures ranging from 250 to 400 °C. Resolvable difference between isotope compositions of surface waters and rocks enables novel insights into boiling, isotope exchange at variable water-rock ratios, and remelting of altered rock. Our measurements of δD, $\Delta'_{17}O$, and $\delta_{18}O$ in well fluids show the reactions proceeded at water-rock ratios of 0.1 to 2, and reveal the addition of meteoric water in the Reykjanes system, and near-surface boiling and steam-liquid separation at Krafla. The $\delta'_{18}O$ and $\Delta'_{17}O$ values of fluids shift due to exchange with rocks at high temperature following the slope 0.51 in the triple isotope space, while boiling causes shifts in δD and $\delta'_{18}O$ values, but does not affect the $\Delta'_{17}O$ fluids significantly due to equilibrium fractionation $\theta_{liquid\text{-}vapor} = 0.529$. Due to small fractionation between epidote and water, epidote $\Delta'_{17}O$ values in all three localities closely resemble the isotope composition of local fluid sources. In meteoric hydrothermal systems, the $\Delta'_{17}O$ of epidotes range between -0.01 and +0.03 ‰, while at seawater-dominated system they are close to that of modified seawater, between -0.02 and +0.01 ‰. The measured slope of triple oxygen isotope fractionation between quartz and epidote at 250-400 °C is 0.526±0.001. The calibrated quartz-water equilibrium fractionation for triple oxygen isotopes yields general agreement with the local fluid sources, within ±1.5 ‰ of their $\delta_{18}O$ values, while the $\Delta'_{17}O$ agree within ±0.02 ‰. We present *in situ* $\delta_{18}O$ measurements in a quartz crystal from Krafla that show

several ‰ heterogeneities which may affect the reconstructed equilibrium fluid values. We tested the effect of shallow crustal contamination on the $\Delta'^{17}O$ values of rhyolitic glasses from Krafla, including those quenched and extracted by drilling, that likely formed by assimilation of low-$\delta^{18}O$ hydrothermally altered crust. Our $\Delta'^{17}O$ measurements constrain the degree of crustal assimilation to 10-20 %. Our study shows that the $\Delta'^{17}O$ values measured in geothermal fluids, secondary minerals and low $\delta^{18}O$ contaminated magmas can provide key information on the conditions of water-rock reaction and magma genesis, and contain additional details that were not accessible through conventional analyses of δD and $\delta^{18}O$.

1. INTRODUCTION

Hydrothermal alteration of mid-ocean ridge basalts to greenschist facies mineral assemblages provides the dominant control on the isotope and elemental budget of seawater and notably modifies the composition of the oceanic crust (Muehlenbachs and Clayton, 1976; Alt and Teagle, 2000). Since, oxygen is the most abundant element both in water and rocks and has a distinct isotope composition in these reservoirs, the alteration can be monitored and quantified by the $^{18}O/^{16}O$ ratio. The advent of high precision triple oxygen isotope measurements enables us to use hydrothermally altered rocks as tracers of fluids in the past and thereby better understand details of past hydrothermal processes. In this paper, we explore the effects of high-temperature alteration of basaltic crust using simultaneous measurements of $^{17}O/^{16}O$ and $^{18}O/^{16}O$ ratios in continental and near-coastal hydrothermal systems of Iceland. We hope to better distinguish the intertwined effects of temperature, fluid isotope composition, mixing of fluids, boiling, and exchange at variable water-rock ratios in controlling the isotope compositions of hydrothermally altered rocks. The systematic mass-dependent relationship between $^{17}O/^{16}O$ and $^{18}O/^{16}O$ in geothermal fluids and minerals reported here promises to provide a variety of useful applications ranging from ore potential and geothermal exploration to studies of ophiolites, paleoclimate proxies, and tracking recycling of isotope compositions through main terrestrial reservoirs.

1.1 Hydrogen and oxygen isotope studies of hydrothermal systems

In areas of extensive magmatism hydrothermal systems are charged with fluids from local sources that move through the crust via convective groundwater flow and react with the host rocks at high temperature (Norton, 1984; Hayba and Ingebrigtsen, 1997; Criss and Taylor, 1986; Manning and Ingebritsen, 1999). Due to high-temperature exchange reactions between fluid and rock, alteration minerals have H- and O-isotope values are close to being in equilibrium

with hydrothermal fluids. The ratios of hydrogen and oxygen isotopes, D/H and $^{18}O/^{16}O$, are widely used to investigate fluid sources, temperature of water-rock interaction and processes that occur in hydrothermal systems such as exchange reactions, boiling, and mixing of various fluid reservoirs (Ohmoto and Rye, 1974; Taylor, 1974; Gregory and Taylor, 1981).

In fossilized hydrothermal system, where fluids are no longer present, measurements of $\delta^{18}O$ values in coexisting mineral pairs, combined with δD measurements of hydrous minerals and fluid inclusion studies, are used for isotope equilibrium calculations involving mineral-mineral and mineral-water calibrations. Combined H- and O-isotope measurements can fingerprint isotope composition of initial fluids (e.g. Taylor, 1974, 1977; Ohmoto and Rye, 1974; Truesdell and Hulston, 1980; Dilles et al., 1992; Giggenbach, 1992; Pope et al., 2014), however the δD values of most hydrous minerals rarely reflect equilibrium with the original hydrothermal fluids at high-temperature (>250 °C) due to subsequent retrogressive exchange at lower temperature (< 100 °C), hydration and weathering (Kyser and Kerrich, 1991; Graham, 1981). Thus, the source of fluids in ancient hydrothermal systems cannot necessarily be determined from $\delta^{18}O$ measurements alone without making assumptions about the isotope composition of fluids or equilibrium temperature. Moreover, the isotope composition of initial fluids can be significantly overprinted due to high-temperature exchange with rocks, varying temperature of alteration, contributions of steam and brine, and addition of magmatic fluids.

Introducing a new isotope parameter $^{17}O/^{16}O$, measured simultaneously with $^{18}O/^{16}O$, enables a new ability to constrain the isotope signature of initial fluids. The unique and systematic relationship between triple oxygen isotope compositions of meteoric waters, seawater and rocks (Landais et al., 2008; Luz and Barkan, 2010; Uemura et al., 2010; Pack and Herwartz, 2014; Sharp et al., 2018) along with recently calibrated equilibrium fractionations (Sharp et al., 2016;

116 Wostrbrock et al., 2018) provide a promising basis to track temperature and O-isotope signature
117 of fluid at the same time. Similarly to $\delta_{18}O$ – δD systematics, the $\delta_{18}O$ - $\delta_{17}O$ systematics of
118 hydrothermal minerals can identify processes that affect isotope composition of the fluid phase,
119 such as boiling, mixing of distinct fluids and isotope exchange with rocks. Unlike combined δD
120 and $\delta_{18}O$ measurements, triple oxygen isotope analyses are obtained concurrently from single
121 aliquots of sample O_2 gas.

122 In this study we investigate the $\delta_{18}O$ - $\delta_{17}O$ relationship in fluids and minerals from active
123 high-temperature (250-400 °C) hydrothermal systems at Reykjanes and Krafla located in
124 southwest and north Iceland, respectively, and at an exposed subvolcanic section in the 6 Ma
125 Geitafell central volcano in southeast Iceland (Fig. 1). These systems serve here as natural
126 laboratories, where distinct fluids with previously determined isotope compositions are reacting
127 with mantle-derived rocks at known temperatures. Using the previous analyses of local
128 precipitation and groundwater recharge sources (Fig. 2) and measurements of fluid pressure and
129 temperature in the geothermal wells, we are able to test the applications of $\Delta'_{17}O$ values under
130 well-defined conditions. We used drill cuttings of quartz and epidote from known depths at
131 Reykjanes and Krafla where temperature in the boiling systems can be determined at specified
132 depth from the boiling point-water depth curve. Quartz and epidote were targeted because their
133 co-occurrence, especially in veins and vesicles, is indicative of hydrothermal alteration at
134 temperatures above 250 °C (Bird and Speiler, 2004), and they are not susceptible to isotope
135 exchange at low temperatures. We also used samples of well fluids from Reykjanes that are
136 dominated by seawater that underwent boiling at depth and isotope exchange with rocks, and
137 from Krafla, where meteoric water boils close to the surface after reaction with rocks at depth.

Measurements from the 6 Ma Geitafell system are used here to validate our findings in the active hydrothermal systems. We test the ability to reconstruct the triple oxygen isotope values of ancient meteoric water at Geitafell similarly to using combined $\delta^{18}O$ and δD values (see Pope et al., 2014). The zoning of alteration minerals and the pattern of isotope ratios in the host rocks of the Geitafell system display a "bull's eye" pattern that formed in response to temperature gradient and circulation of meteoric water around the cooling intrusion (Taylor and Forester, 1979). This study is also a next logical step in validating previous triple oxygen isotope investigations of ancient hydrothermally altered rocks (Herwartz et al., 2015; Zakharov et al., 2017; Zakharov and Bindeman, 2019). Those investigations applied the triple oxygen isotope approach to resolve ancient environment conditions using lithologies that experienced aqueous alteration billions of years ago. Since the triple oxygen isotope composition of high-temperature minerals is not easily reset, even during regional metamorphism, the current paper provides basis for validating the findings in those previous studies.

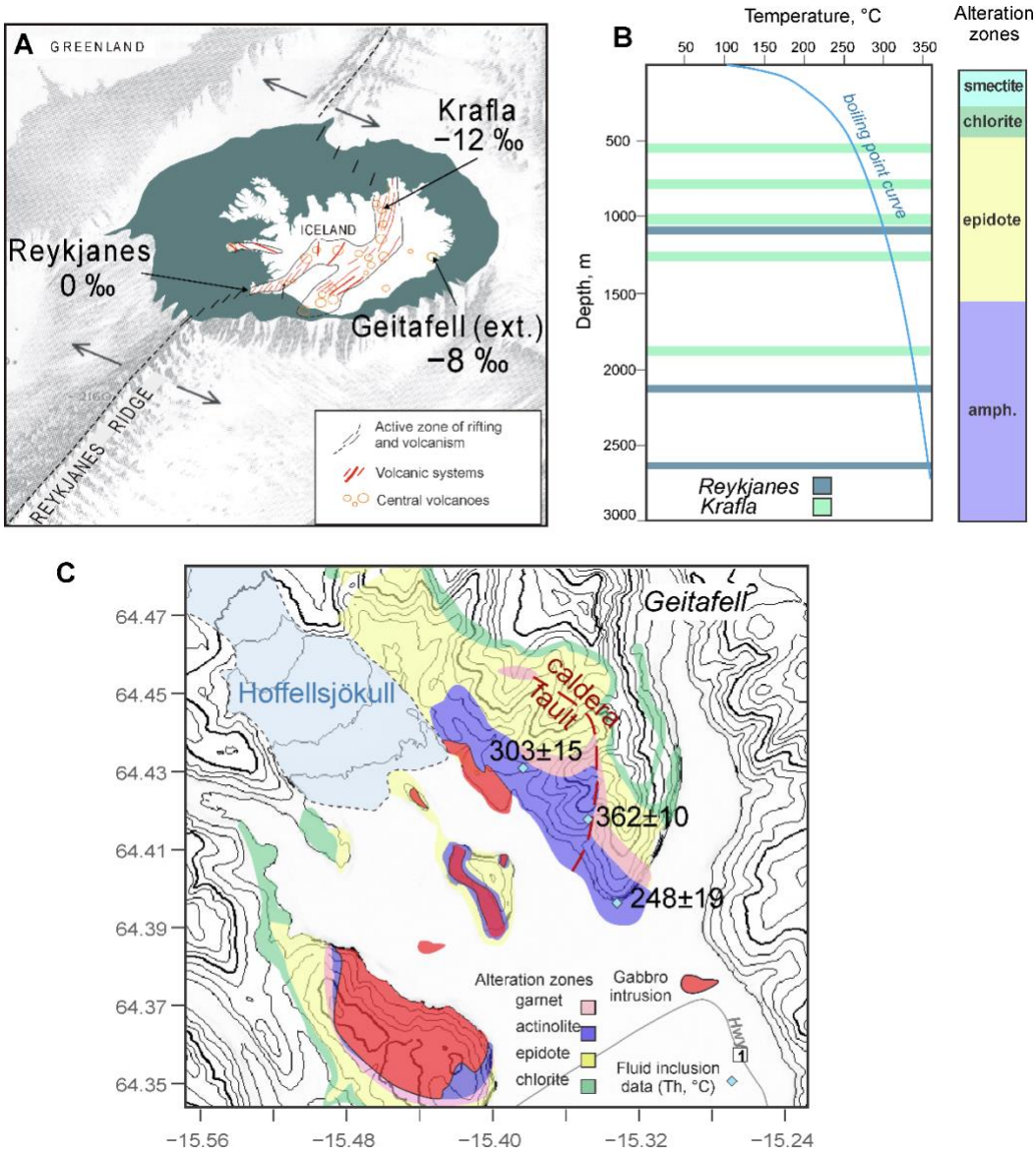

Figure 1. (A) Locations of the geothermal systems of Iceland studied here. The Reykjanes and Krafla systems are currently active, while the 6 Ma Geitafell extinct volcano hosts a fossilized hydrothermal system eroded to the depth of about 2 km (Friðleifsson, 1983). (B) The temperature of alteration for Reykjanes and Krafla systems can be approximated by the boiling point of water at depth. The temperatures are consistent with characteristic alteration mineral zones from top to bottom: smectite, chlorite, epidote and amphibole. The depth of collected samples is shown with horizontal bands. (C) General pattern of alteration at the Geitafell subvolcanic system. The gabbro intrusion is surrounded by a concentric pattern of alteration zones (Friðleifsson, 1983; Thorlacius, 1991) similar to the ones observed in the downward profiles recovered from drill holes in the modern hydrothermal systems. The average homogenization temperature (Th, °C in the legend) of fluid inclusions measured in quartz veins

surrounding the intrusion is shown with blue diamonds (after Troyer et al., 2007). These values were used as an approximate estimate of temperature of quartz-water equilibrium for corresponding samples (GER16 and GER34 in Table 1). Topographic contour lines are drawn every 100 m. White area represents elevation of about 5 meters above sea level.

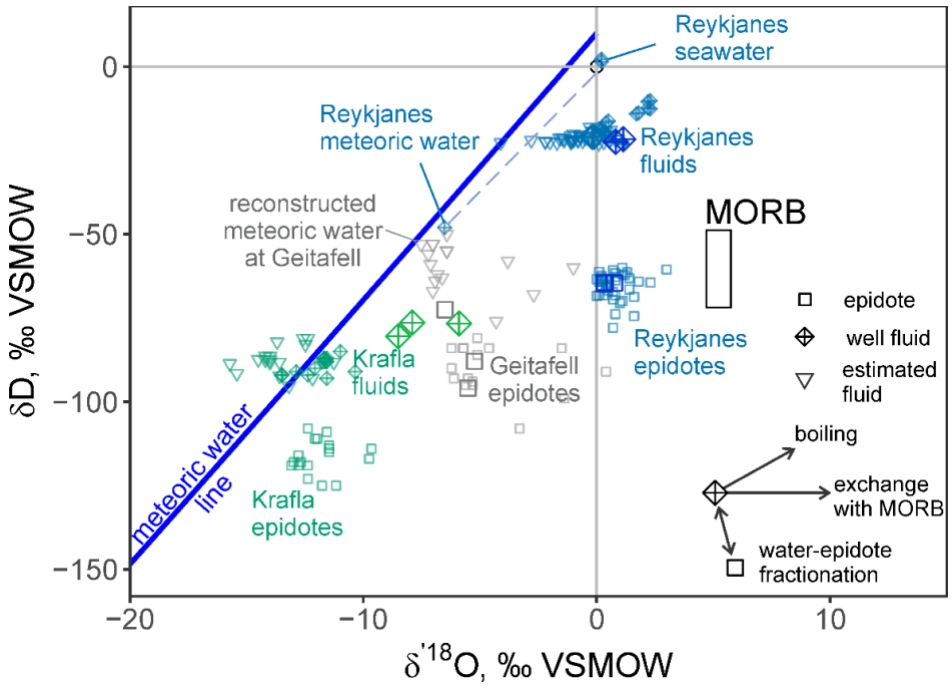

Figure 2. Compiled δD and $\delta_{18}O$ data for well fluids and epidotes at the Reykjanes, Krafla and Geitafell systems. The data gathered from Pope et al. (2011; 2014; small symbols) and multiple measurements from this study (large symbols). The Reykjanes fluids are derived from seawater ($\delta_{18}O$ and δD = 0 ‰) with minor amount of local meteoric water with $\delta_{18}O$ of -6.5 ‰ (Ólafsson and Riley, 1978). Krafla fluids are derived from meteoric water with $\delta_{18}O$ of -13 ‰ and δD of -90 ‰. Geitafell epidote indicates meteoric waters with $\delta_{18}O$ of about -8 ‰. Compositional field of mid-ocean ridge basalt (MORB) represents initial unaltered rock. Isotope shifts experienced by hydrothermal fluids and water-epidote fractionation are shown schematically in the lower right corner.

1.2 $\delta'_{18}O$ and $\Delta'_{17}O$ definition

Mass-dependent fractionation of triple oxygen isotopes between entities A and B obeys the relationship (Urey, 1947; Matsuhisa et al., 1978; Cao and Liu, 2011):

$$ln\,^{17}\alpha_{A-B} = \theta \cdot ln^{18}\alpha_{A-B} \quad (1),$$

where $^{17,18}\alpha_{A\text{-}B}$ are the ratios of $^{17}O/^{16}O$ or $^{18}O/^{16}O$ in A to that in B. The value of θ, the triple isotope exponent, is a temperature-dependent variable typically ranging between 0.5 and 0.5305 for equilibrium and kinetic processes (Matsuhisa et al., 1978; Cao and Liu, 2011; Hayles et al., 2017). Since the relationship between $^{17}\alpha$ and $^{18}\alpha$ is exponential, we adopt linearized delta notation expressed through natural logarithm and denoted by a prime symbol (′) (Miller, 2002):

$$\delta'\,^{x}O = 1000ln\,(1 + \frac{\delta\,^{x}O}{1000}) \quad (2),$$

where *x* is either 17 or 18. The $\delta_x O$ value in Eq. 2 is the conventionally defined delta-notation:

$$\delta\,^{x}O = 1000(\frac{{}^{x}O/{}_{^{16}O_{sample}}}{{}^{x}O/{}_{^{16}O_{VSMOW}}} - 1) \quad (3),$$

where VSMOW (Vienna Standard Mean Oceanic Water) represents a standard with isotope ratios close to that of seawater. Using the linearized notations for triple oxygen isotope fractionation, the θ value can be expressed as a slope in the $\delta'^{17}O - \delta'^{18}O$ coordinates:

$$\theta = \frac{\delta'^{17}O_A - \delta'^{17}O_B}{\delta'^{18}O_A - \delta'^{18}O_B} \quad (4),$$

where A and B are two substances in equilibrium, for example quartz and water, quartz and epidote. When measuring fractionations in triple oxygen isotope system, instead of using the slopes in $\delta'^{18}O - \delta'^{17}O$ coordinates, it is more illustrative to use $\Delta'^{17}O$ notation, often termed ^{17}O-excess. Deviations of $\delta'^{17}O$-$\delta'^{18}O$ fractionations from a reference line with slope of λ_{RF} are then expressed as $\Delta'^{17}O$:

$$\Delta'^{17}O = \delta'^{17}O - \lambda_{RF} \cdot \delta'^{18}O \quad (5).$$

Following definitions in previous studies of silicate rocks and precipitation (e.g., Landais et al., 2008; Luz and Barkan, 2010; Pack et al., 2016), in the Eq. 5 we use the reference line with the slope of $\lambda_{RF} = 0.528$.

1.3 Isotope signals in hydrothermal systems

The δD, $\delta_{18}O$ and $\Delta_{17}O$ values of fluids and rocks in hydrothermal systems are distinctive owing to evaporation and condensation that surface waters undergo. Since VSMOW is used as a standard for the definition of δD, $\delta_{18}O$ and $\Delta_{17}O$, all three values are close to 0 ‰ in modern seawater. In the globally averaged meteoric water, hydrogen and oxygen isotopes are related through the equation also known as the global meteoric water line (Craig, 1961):

$$\delta D = 8 \cdot \delta^{18}O + 10 \quad (6).$$

Likewise, the $\delta'_{17}O$ value in meteoric water is related to the $\delta'_{18}O$ through the effects of water-vapor fractionation and relative humidity (Luz and Barkan, 2010). As shown in the recent compilation of meteoric water values (Sharp et al., 2018), the traditionally used single meteoric water line with the slope of 0.528 and y-intercept of 0.033 in $\delta'_{17}O$-$\delta'_{18}O$ coordinates (Luz and Barkan, 2010) may not be representative of precipitation globally. Using the compilation from Sharp et al. (2018), we approximate the slope and y-intercept of meteoric water line by fitting a linear regression across the range of $\delta'_{18}O$ values between -40 and 0 ‰. The linear regression yields coefficients:

$$\delta'^{17}O = 0.5272(0.0001) \cdot \delta'^{18}O + 0.016(0.002) \quad (7),$$

with standard errors given in parenthesis. This equation takes into account the diversity of processes that compose isotope signature of meteoric waters (reevaporation, humidity and water-vapor fractionation) including hydrologic cycle in the high-latitude regions such as Iceland.

Combined with Eq. (5), triple oxygen isotope meteoric water line in coordinates specific for any reference slope can be expressed through $\Delta'^{17}O$:

$$\Delta'^{17}O = (0.527 - \lambda_{RF}) \cdot \delta'^{18}O + 0.016 \quad (8).$$

We use these global meteoric water relationships (Fig. 3) to approximate the isotope composition of precipitation at the localities studied here. Using the global $\delta^{18}O$ – δD relationship is a strong assumption since the correlation between these values in meteoric waters is very tight ($r^2 > 0.95$; see Craig, 1961) and previous studies showed that the local precipitation is very close to the global meteoric water line (Árnason, 1976). As for the $\delta'^{18}O$ - $\Delta'^{17}O$ relationship, we report 95 % prediction intervals resulting in a meteoric water "band". This is done to emphasize the poor fit ($r^2 = 0.23$) of the linear regression line caused by the scatter in the $\Delta'^{17}O$ of meteoric waters across the range of $\delta'^{18}O$ values (see Fig. 3B). Using the prediction intervals allows us to consider the possible variability within the original local precipitation caused by local isotope effects (e.g. relative humidity, re-evaporation, water-vapor fractionation) when we sample the well fluids or when we derive equilibrium fluid values from mineral analyses.

In each of the three localities, water-rock interaction involved distinctly different reservoirs of surface waters – meteoric water and seawater – reacting with basaltic rocks that have relatively uniform H- and O-isotope composition (Hattori and Muehlenbachs, 1982; Eiler, 2001). The triple oxygen isotope compositions of these reservoirs differ due to small but systematic mass-dependent variations in fractionation of $^{17}O/^{16}O$ relative to $^{18}O/^{16}O$. Mantle rocks have negative $\Delta'^{17}O$ values ranging between −0.06 and −0.05 ‰ (Herwartz and Pack, 2014; Pack et al., 2016) with δD values of -70 ± 10 ‰ (Kyser and O'Neil, 1984; Dixon et al., 2017). The effect of isotope exchange between rocks and fluids at high temperature leads to shifts in the $\delta^{18}O$ and $\Delta'^{17}O$ values of the fluids, and to a lesser extent, in their δD values. We show associated isotope

245 shifts in fluids and its effect on equilibrium quartz and epidote (Fig. 3). In addition, liquid-vapor
246 separation and mixing between seawater and meteoric water affects the stable isotope
247 composition of the fluids and minerals in shallow continental systems (Fig. 3).
248 The Reykjanes, Krafla, and Geitafell systems have well characterized δD and $\delta^{18}O$
249 compositions of the hydrothermal fluids, local fluid sources and alteration minerals (Fig. 2;
250 Árnason, 1976; Ólafsson and Riley, 1978; Sveinbjornsdottir et al., 1986; Darling and
251 Ármannsson, 1989; Pope et al., 2014; Pope et al., 2016). Reykjanes is a seawater-dominated
252 hydrothermal system where fluids have salinity of local seawater and $\delta^{18}O$ close to those of
253 seawater, with average value of −1.1 ‰ and the δD of about −23 ‰ reflecting a contribution
254 from steam and a small addition of local meteoric water (Ólafsson and Riley, 1978; Pope et al.,
255 2009). At Krafla, the meteoric-derived fluids have $\delta^{18}O$ values close to those of local
256 precipitation, ranging between −13 and −12 ‰, and δD values between −94 and −87 ‰ (Darling
257 and Ármannsson, 1989; Pope et al., 2016). Geitafell has a multi-phase intrusion of gabbro and a
258 several-kilometer radius areole of hydrothermally altered tholeiitic lavas (Friðleifsson, 1983)
259 where Pope et al. (2014) measured δD and $\delta^{18}O$ in epidote and determined that hydrothermal
260 fluids were derived from meteoric water with $\delta^{18}O$ of about −8 ± 1 ‰ and δD of about −60 ± 10
261 ‰.
262

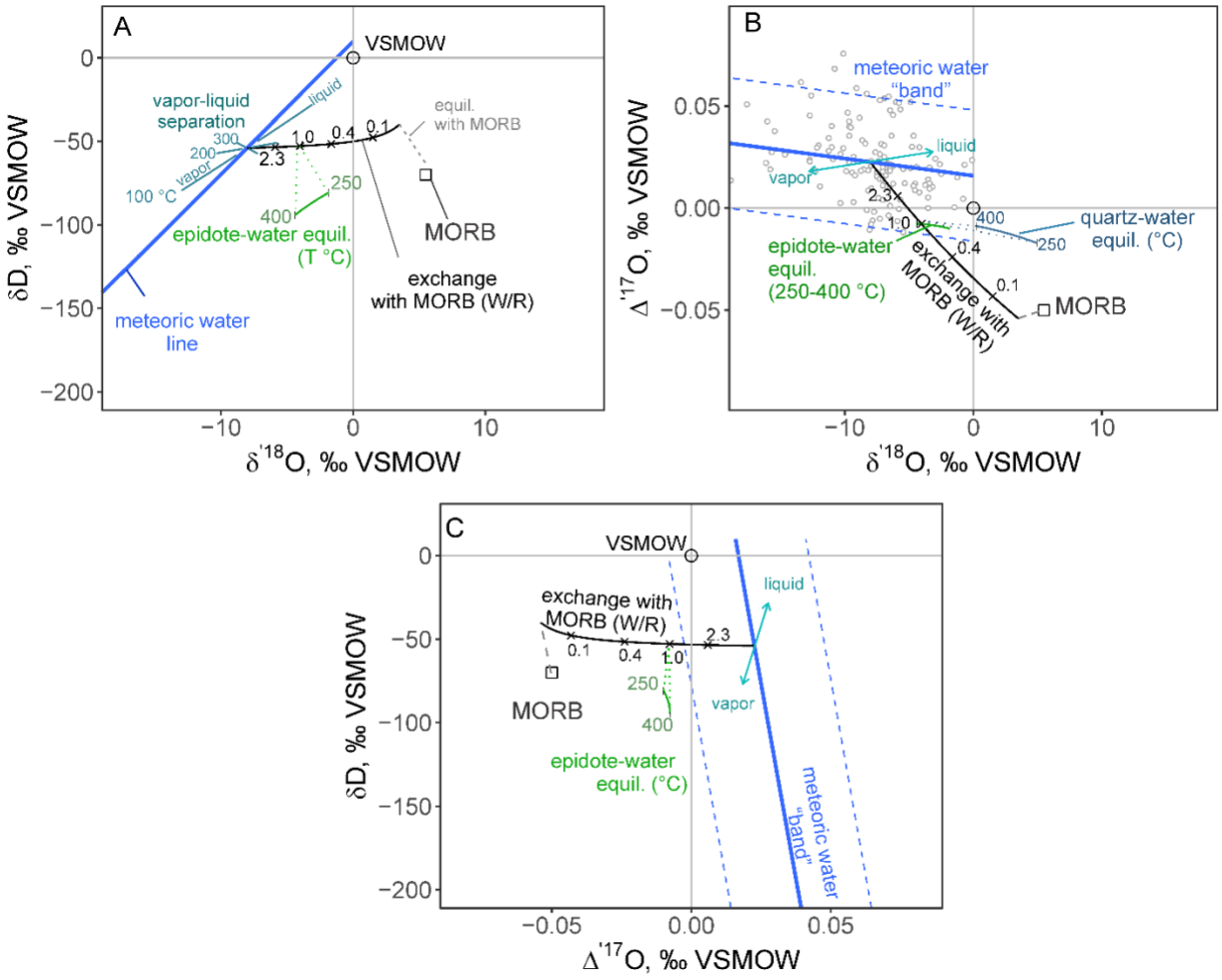

263

264 **Figure 3.** Systematics of water-rock interaction between meteoric water and mid-ocean ridge basalt
265 (MORB) for the three stable isotope parameters plotted in coordinates: conventional δD-δ_{18}O (A), δ'_{18}O –
266 Δ'_{17}O (B) and Δ'_{17}O-δD (C). The processes of isotope exchange (solid black line), boiling (blue straight
267 lines), quartz-water fractionation (light blue curve) and epidote-water fractionation (green curve) at 250-
268 400 °C are depicted for interaction between unaltered MORB and pristine meteoric water that has δ'_{18}O of
269 -8 ‰ (on the global meteoric water line, Craig, 1961). Meteoric water "band" refers to the regression line
270 (solid blue) and 95 % prediction intervals (dashed blue) that are based on the compilation of Δ'_{17}O values
271 in meteoric waters (open grey circles in B; Luz and Barkan, 2010; Sharp et al., 2018 and references
272 therein). Tick marks on the solid black line and numbers indicate water-rock ratios (W/R) of isotope
273 exchange reactions. Quartz-water equilibrium at 250-400 °C is after (Sharp et al., 2016). Epidote-water
274 equilibrium slope is approximated by the quartz-water fractionation at high temperature (>250 °C; see
275 Methods).
276

2 METHODS

2.1 Oxygen isotope measurements

All stable isotope analyses of solids were carried out at the University of Oregon Stable Isotope Lab. For oxygen isotope analyses we used quartz and epidote from all three localities, volcanic glasses from Krafla well IDDP-1 and surface exposures (sample KRF14), and one sample of hydrothermal garnet from Geitafell. All samples were examined with a stereo microscope for inclusions of other minerals prior to analysis. Small samples (1.5-2 mg) were placed in a vacuum chamber and pre-treated with BrF_5 overnight to remove the absorbed moisture and reactive compounds. The oxygen was liberated from the samples by heating them with a CO_2 laser in presence of BrF_5. Extracted oxygen was transported in a stainless steel ¼-inch tube vacuum line, and traces of remaining reagent and other fluorine-containing byproducts were removed by cryogenic traps and reaction with Hg-vapor in a mercury diffusion pump. After the purification, oxygen gas was trapped on a 5Å molecular sieve by cooling to liquid nitrogen temperature. Subsequently released, the gas was carried though a GC-column by He-flow at the rate 30mL/minute and room temperature. After about 3 minutes of elution time, oxygen gas was trapped on a 5Å molecular sieve immersed in liquid nitrogen. The gas was further trapped on another, smaller volume 5Å molecular sieve immersed in liquid nitrogen and introduced into a MAT 253 gas-source isotope-ratio mass spectrometer at 50-60 °C. Each measurement consisted of at least 24 cycles of sample-reference gas comparisons with intermittent equilibration of pressure in the bellows of the mass spectrometer (see Methods in Bindeman et al., 2018; Zakharov and Bindeman, 2019). A subset of samples collected from the Geitafell extinct volcano was analyzed for $^{18}O/^{16}O$ ratio only via conversion of O_2 gas to CO_2 in a heated platinum-graphite converter for a more rapid analysis.

The measurements of well fluids were carried out at the IPM, Okayama University, Japan using fluorination line with a Ni-reactor tube. A few microliters of fluid samples were injected into the reactor and fluorinated using BrF_5 at 250 °C to liberate O_2 gas. The rest of the procedure can be found in Tanaka and Nakamura (2013).

The $\delta_{18}O$ and $\delta_{17}O$ of fluid samples were calibrated to the VSMOW2-SLAP2 scale using the VSMOW2 ($\delta_{18}O_{VSMOW2} \equiv 0 \pm 0.124$ and $\delta_{17}O_{VSMOW2} \equiv 0 \pm 0.070$, N = 5, 2SD) and SLAP2 ($\delta_{18}O_{VSMOW2} = -55.283 \pm 0.226$ and $\delta_{17}O_{VSMOW2} = -29.572 \pm 0.141$, N = 3, 2SD) values measured during this study at the Okayama University. The $\delta'_{18}O$ and $\Delta'_{17}O$ values of silicates were measured at the University of Oregon using the reference gas that has values $\delta_{17}O = 12.042 \pm 0.067$ ‰ and $\delta_{18}O = 23.587 \pm 0.084$ ‰ (mean ± 2SD). These values were determined by analyzing it against the VSMOW2-SLAP2-calibrated reference gas at the IsoLab, University of Washington. Since we did not measure VSMOW2 and SLAP2 during analyses of silicates, we used San Carlos olivine (SCO) as an internal standard within each session to monitor the accuracy. As reported previously (Pack et al., 2016), the SCO values are $\delta'_{17}O = 2.677 \pm 0.086$ ‰ and $\delta'_{18}O = 5.140 \pm 0.161$ ‰ (mean ± 1SD) calibrated to VSMOW2-SLAP2 scale. Each analysis was adjusted to the difference between these and measured values of SCO within the session. The uncorrected values reported against the reference gas are assembled in Supplementary Table 1. The measurements of SCO (n=9) yielded $\delta'_{17}O = 2.890 \pm 0.185$ ‰ and $\delta'_{18}O = 5.606 \pm 0.301$ ‰ (mean ± 1SD).

We also measured $\delta_{18}O$ values *in situ* in a quartz crystal extracted from the Krafla well KJ36 at depth of 744 m using a secondary ion mass spectrometer (SIMS) CAMECA IMS-1280 at the WiscSIMS lab, University of Wisconsin. First, a polished section of quartz was imaged using a FEI Quanta field emission gun scanning electron microscope equipped with a

323 cathodoluminescence (CL) grayscale detector at the University of Oregon. The $\delta_{18}O$ values were
324 analyzed from 10-µm-diameter spots by SIMS. A polished grain of UWQ-1 quartz standard ($\delta_{18}O$
325 = 12.33 ‰; Kita et al., 2009) was mounted with the samples and used as a bracketing standard.
326 The precision during the analyses was ± 0.4 ‰ or better (2 standard errors).

327 ***2.2 Hydrogen isotopes***

328 Hydrogen isotopes were analyzed using a high temperature thermal conversion elemental
329 analyzer (TC/EA) that is connected to the MAT 253 at the University of Oregon, using a
330 continuous flow mode where gases from samples and standards are transported in He carrier gas
331 (see methods in Hudak and Bindeman, 2018). Each solid sample and standard were wrapped in a
332 silver foil capsule and dried in a vacuum oven overnight, then transported to the auto sampler
333 where they were purged with He carrier gas. In the TC/EA's furnace lined with a glassy carbon
334 column, samples experienced pyrolysis at 1450 °C, and all of the H_2O in the minerals was
335 pyrolized to H_2 and CO gas. Extracted gas carried by He into a gas chromatograph where H_2 is
336 resolved from CO, which was discarded. The CONFLOIII device was used to lower the sample
337 pressure to atmospheric, suitable for introduction into the mass spectrometer, which also meters
338 pulses of monitoring gas. Mica standards, USGS57 and USGS58 (δD = −91 and −28 ‰,
339 respectively; Qi et al., 2017) were included in each analytical session to monitor the accuracy of
340 analysis. The δD values of fluid samples were determined using the same TC/EA set up through
341 multiple injections directly into the glassy carbon column.

342 ***2.3 Equilibrium fractionation calculations***

343 We used the calibrations by Sharp et al., (2016) and Wostbrock et al., (2018) to derive the
344 $\delta'_{18}O$ values of equilibrium fluids using measurements of quartz:

345 $$\delta'^{18}O_{quartz} - \delta'^{18}O_{water} = \frac{4.28 \pm 0.07 \times 10^6}{T^2} - \frac{3.5 \pm 0.2 \times 10^3}{T} \quad (9),$$

and the $\Delta'^{17}O$ of equilibrium fluids:

$$\Delta'^{17}O_{quartz} - \Delta'^{17}O_{water} = \left(\frac{4.28 \pm 0.07 \times 10^6}{T^2} - \frac{3.5 \pm 0.2 \times 10^3}{T}\right) \times \left(0.5305 - \frac{1.85 \pm 0.02}{T}\right) \quad (10),$$

where T is equilibrium temperature in Kelvins. At 250-400 °C, fractionation is such that $\delta'^{18}O_{quartz} - \delta'^{18}O_{water}$ and $\Delta'^{17}O_{quartz}$-$\Delta'^{17}O_{water}$ is about +4-9 ‰ and −0.04 to −0.01 ‰ respectively. At this temperature range, epidote has $\delta^{18}O$ values within ±1.5 ‰ of the equilibrium fluids (Zheng, 1993). The approximate $\Delta'^{17}O$ fractionation for epidote-water could be derived from Eq. 10 by substitution of the first term with the incremental calibration of $^{18}O/^{16}O$ ratio given by Zheng, 1993:

$$\Delta'^{17}O_{epidote} - \Delta'^{17}O_{water} = \left(\frac{4.05 \times 10^6}{T^2} - \frac{7.81 \times 10^3}{T} + 2.29\right) \times \left(0.5305 - \frac{1.85 \pm 0.02}{T}\right) \quad (11).$$

In general, the $\Delta'^{17}O_{mineral}$-$\Delta'^{17}O_{water}$ fractionation is expected to approach the high-temperature fractionation limit with increasing temperature, though at different rates for different mineral species. In this study, the second term in Eq. 11 is borrowed from quartz-water fractionation (Eq. 10). Even though that part of equation has not been calibrated for epidote-water fractionation and the factor -1.85 is likely not correct, we assume that it may serve as a valid approximation for the high-temperature systems (250-400 °C), where triple oxygen isotope fractionation approaches its high-temperature limit. From the equations 10 and 11 it is clear, when the T is high, the second term (or θ value in Eq. 4) approaches 0.5305 (Matsuhisa et al., 1978; Bao et al., 2016; Hayles et al., 2018).

To provide an additional estimate of the temperature of alteration in the Geitafell fossilized hydrothermal system, we used the empirical calibration for quartz-epidote equilibrium fractionation given in Matthews (1994):

$$1000ln^{18}\alpha_{quartz-epidote} = \delta'^{18}O_{quartz} - \delta'^{18}O_{epidote}$$

$$= (2 + 0.75 \times Xps)10^6/T^2 \quad (12),$$

where X*ps* is mole proportion of pistacite in epidote, calculated as the proportion of iron in formula coefficient units, $Fe^{3+}/(Al+Fe^{3+})$. We used the X*ps* value of 0.2, which is an average value based on previous measurements for Krafla and Reykjanes epidotes (see Sveinbjornsdottir, 1991).

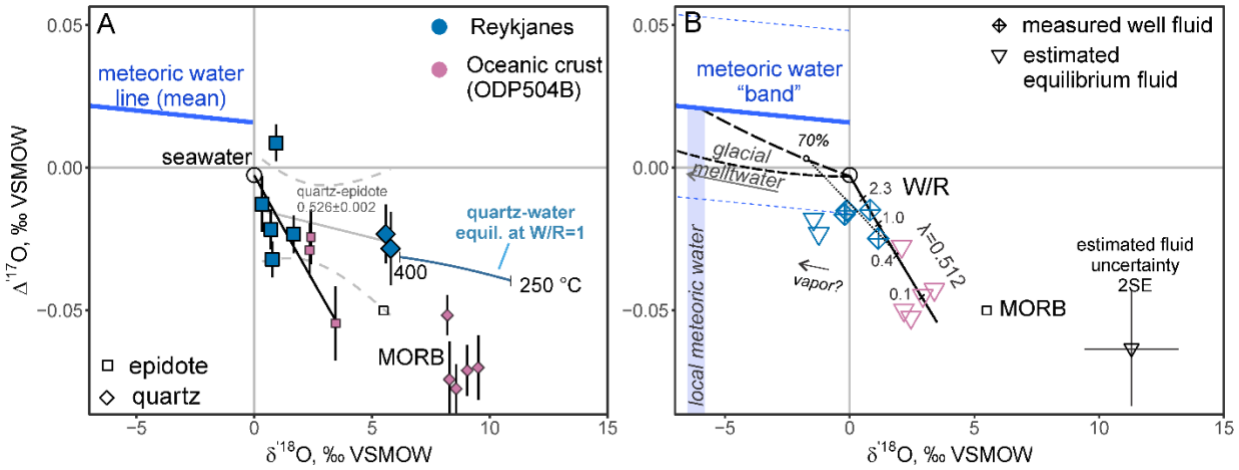

Figure 4. Triple oxygen isotope values of minerals (A) and fluids (B) from Reykjanes. A – Values plotted for quartz and epidote from Reykjanes, and from modern oceanic crust as sampled by the drill hole ODP 504B in east Pacific Ocean (shown for comparison; Zakharov and Bindeman, 2019). The apparent fractionation of triple oxygen isotopes between quartz and epidote at Reykjanes is shown with grey line and 95% confidence intervals (dashed). Quartz-water equilibrium at 250-400 °C is shown with the blue curve (Sharp et al., 2016). B – Values plotted for estimated equilibrium fluids computed from quartz-water fractionation (Eq. 10) and for well fluids measured directly. For both Reykjanes and modern oceanic crust, seawater, shown with an open circle, is the dominant fluid involved in alteration of mid-ocean ridge basalts (MORB). The seawater exchanged with rocks at high temperature becomes higher in $\delta'^{18}O$ and lower in $\Delta'^{17}O$ following the slope of $\lambda = 0.512$ in $\delta'^{17}O - \delta'^{18}O$ space (black solid curve). Mixing line with local meteoric water at Reykjanes is shown as a dashed curve with maximum percent fraction of local meteoric water. Contribution of vapor phase is shown with an arrow.

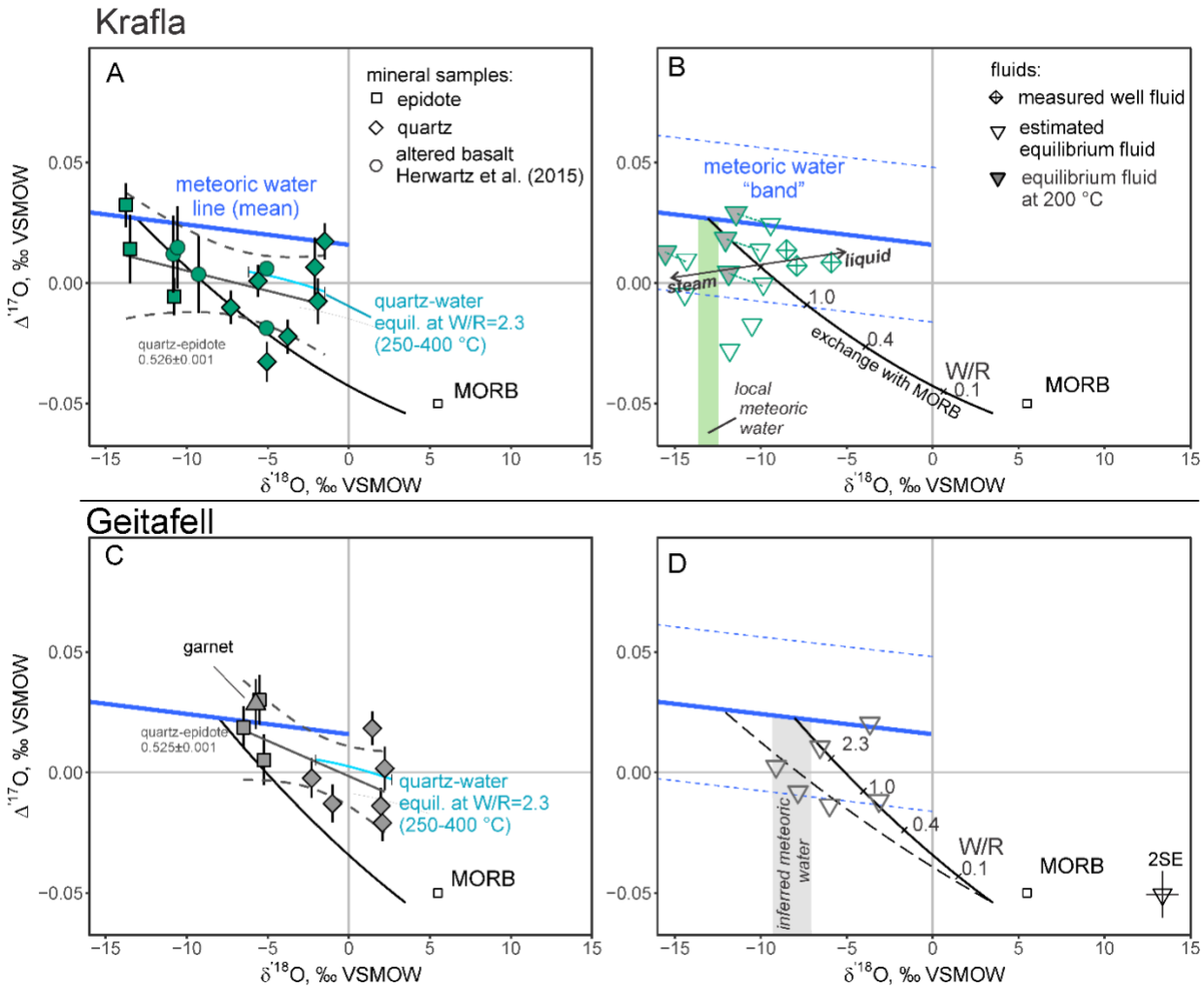

Figure 5. The $\delta'_{18}O - \Delta'_{17}O$ values of minerals (A and C) and fluids (measured and computed; B and D) from Krafla and Geitafell systems. The apparent fractionation of triple oxygen isotopes between quartz and epidote is shown with grey line and 95% confidence intervals (dashed). The vertical bands on the right panels show the $\delta'_{18}O$ values of local fluid sources (measured directly or inferred from δD values). Additionally, exchange with meteoric water that composition of modern precipitation at Krafla is shown for Geitafell with dashed curve. The well fluids at Krafla system originated from exchange with rocks and liquid-vapor separation, which is reflected by their high $\delta'_{18}O$ values with $\Delta'_{17}O$ similar to those computed from quartz-water equilibrium. The estimated equilibrium fluids were computed using the boiling point of water at collection depth and the 4 samples of quartz collected at shallow depth (<1000m) at Krafla systems were used to calculate equilibrium fluids (grey-filled symbols) at the temperature of local thermocline of 200 °C (Sveinbjornsdottir et al., 1986).

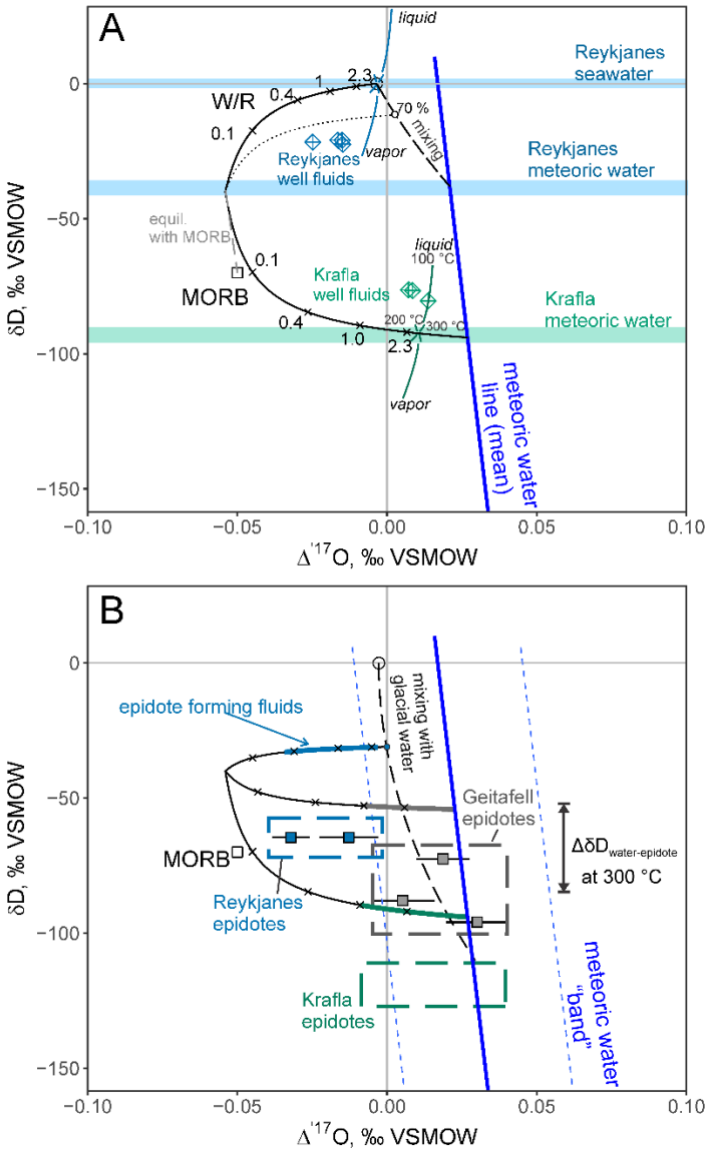

Figure 6. Combined $\Delta'_{17}O$ and δD measurements of well fluids (A) and epidotes (B). A - The Reykjanes well fluids are best explained by small contribution of local meteoric water, subsurface boiling and isotope exchange with rocks. Krafla fluids represent residual liquid fraction after steam separation, which explains the heavy δD values compared to the exchange trend. B – The $\Delta'_{17}O$ and δD values of epidotes are shown as boxes (compiled data from here and Pope et al., 2014). Where combined measurements are available for the same sample, the values are shown with square symbols. At Geitafell these values are consistent with the reconstructed meteoric water ($\delta_{18}O$ of -8 ‰), while epidotes from Reykjanes may record contribution of low $\delta_{18}O$ and δD glacial waters (see Pope et al., 2009). Krafla epidotes reflect equilibrium fluids close to pristine local meteoric water.

3 RESULTS

3.1 *Measured δ′$_{18}$O, Δ′$_{17}$O and δD values*

The δ′$_{18}$O, Δ′$_{17}$O and δD values of minerals and well fluids from Reykjanes and Krafla and mineral separates from Geitafell are reported in Table 1. Quartz, epidote, measured well fluids and estimated equilibrium fluids are graphically presented in Figures 4, 5 and 6.

The Δ′$_{17}$O values of Reykjanes well fluids range between -0.03 and -0.02 ‰, in general agreement with seawater-dominated origin of the fluids. The three measurements of Krafla fluids, that range in δ′$_{18}$O between -8 and -6 ‰, are several ‰ higher than the local precipitation (δ′$_{18}$O = -13 ‰) since they represent the remaining liquid of the fluids that underwent boiling and steam-liquid separation in the near surface environment (Ármannsson et al., 2014; Pope et al., 2016). One samples has a high δ′$_{18}$O value of -5.9 ‰. This sample (Krafla pool; Table 1) represents the power plant discharge at Krafla. The Krafla fluid samples have distinctly high Δ′$_{17}$O values of about +0.01 ‰.

The δ′$_{18}$O and Δ′$_{17}$O values of Reykjanes epidotes are close to seawater values, varying between 0 and +1 ‰, and -0.03 and +0.01 ‰ respectively (Fig. 4). The Krafla epidotes have low δ′$_{18}$O values, between -14 and -11 ‰, and high Δ′$_{17}$O values of -0.01 and +0.03 ‰. Geitafell epidotes have δ′$_{18}$O values between -7 and -5 ‰, and Δ′$_{17}$O values between +0.01 and +0.03 ‰. The quartz samples are consistent with equilibrium fractionation at the temperature range between 250 and 400 °C being about 5-9 ‰ higher than the well fluids and epidotes. Their Δ′$_{17}$O values are about 0.01-0.03 ‰ lower than the respective fluid sources and epidotes (Figs 4 and 5). Our measurements constrain apparent fractionation of triple oxygen isotopes between quartz and epidote as shown in the Eq. 4. The mean and standard error of the slope in δ′$_{17}$O-δ′$_{18}$O coordinates is 0.526 ± 0.001 and shown for each locality along with the 95 % confidence

intervals (Fig. 4 and 5). This value corresponds to measured fractionation at the temperature range 250-400 °C and does not necessarily represent equilibrium fractionation between the two minerals.

In this study, we used a silicate standard (SCO) that has $\delta'^{18}O$ value about 20 ‰ higher than the lowest values measured in Krafla epidotes. It would be a good practice for future workers to develop a low $\delta^{18}O$ silicate standard with the $\Delta'^{17}O$ value calibrated to SLAP2-VSMOW2 scale. In such case the values reported here could be corrected for a possible scale distortion effect using the values in Supplementary Table 1 and the reference gas value (see Methods section). The documented examples of scale distortions in other mass spectrometers show that the difference between true and measured $\Delta'^{17}O$ values is on the order of 0.001 - 0.050 ‰ for the 60 ‰ $\delta'^{18}O$ range of the VSMOW2-SLAP2 scale (Schoenemann et al., 2013; Pack et al., 2016; Yeung et al., 2018). We suggest that the measurements used here are appropriate for studying hydrothermal processes because of the following reasons: i) the span of $\delta'^{18}O$ in studied samples is less extreme than the VSMOW2-SLAP2 range; ii) the fluid samples reported here are calibrated to VSMOW2- SLAP2 and their values compare well the mineral data.

3.2 Computed equilibrium fluids

Using the boiling point-depth to estimate temperature, the $\delta'^{18}O$ values of equilibrium fluids were computed based on quartz measurements and the Eq. 9 and 10 (Sharp et al., 2016; Wostbrock et al., 2018). The uncertainty of $\delta'^{18}O$ and $\Delta'^{17}O$ values of equilibrium fluids was estimated by propagating the uncertainties in fractionation factors and the analytical errors through the equations 9 and 10. We used the average values of analytical standard errors (SE): 0.005 ‰ for $\delta'^{18}O$ and 0.010 ‰ for $\Delta'^{17}O$. The uncertainty of ±30 °C was used as the largest possible error on the temperature estimate given by the variations in the well log measurements.

460 The resulting propagated uncertainty of equilibrium fluids are 1.151 ‰ for $\delta'^{18}O$ and 0.011 ‰
461 for $\Delta'^{17}O$ (1SE). It is worth mentioning that the equilibrium fractionation of $\Delta'^{17}O$ values
462 between water and quartz at temperature is not resolvable in the range 350-400 °C due to
463 analytical uncertainty of ~0.01 ‰.

464 ***3.3 In situ $\delta^{18}O$ measurements of Krafla quartz***

465 The cathodoluminescence (CL) image and the heterogeneous $\delta^{18}O$ values measured *in situ* in
466 a quartz crystal from Krafla are shown on Fig. 7A. The CL-pattern reveals features indicative of
467 precipitation at different temperature manifested by different brightness (Fig. 7A). The $\delta^{18}O$
468 values measured *in situ* vary between -2 and 0 ‰ for most of the crystal, while the some of the
469 CL-dark outermost rims are about -4 ‰. We show the effect of decreasing temperature and
470 evolving fluids on the triple oxygen isotope composition of equilibrium quartz in Figure 7B.

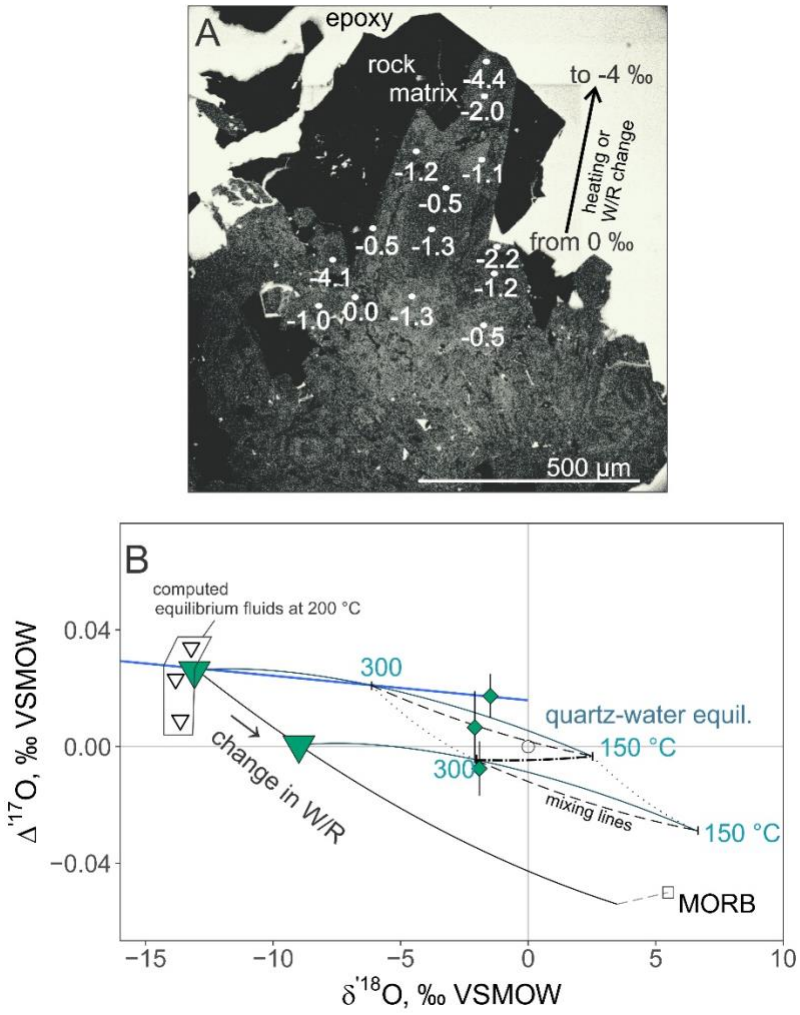

471

472 **Figure 7.** A – Cathodoluminescent image of quartz (grey; center) from Krafla collected at depth of 744 m
473 and analyzed by SIMS for oxygen isotopes. The $\delta_{18}O$ values (shown in white) vary from -4 ‰ to about
474 0 ‰, which translates to temperature change from 190 to 270 °C assuming a fixed value of equilibrium
475 fluids ($\delta'_{18}O$ = -13 ‰). B – The combined effect of variable temperature and variable water-rock ratio
476 (W/R) on the triple oxygen isotope composition of equilibrium quartz. The two concave down curves
477 indicate equilibrium fractionation between quartz and two arbitrarily chosen shifted fluid compositions
478 (filled triangles). The tick marks on the curves show quartz compositions at 150 and 300 °C. Mixing
479 between equilibrium compositions are shown with dashed (variable temperature, fixed W/R), dotted
480 (variable W/R, fixed temperature) and dashed-dotted (variable temperature, variable W/R) curves. The
481 reconstructed equilibrium fluids at 200 °C based on measurements of quartz from Krafla (collected at
482 depth 744 m) are shown with open triangles.
483

3.4 Distribution of $\delta'^{18}O$ values at the Geitafell system

In addition to the triple oxygen isotope measurements, we present the spatial distribution of $\delta'^{18}O$ values measured in quartz and epidote separates from Geitafell. The values are reported in Supplementary Table 2. The value of $\delta'^{18}O_{quartz}$ - $\delta'^{18}O_{epidote}$ ranges between 5 and 10 ‰, approaching the minimum near the contact of the Geitafell intrusion (Fig. 8). This range of fractionation is consistent with the temperature of alteration between 200 and 450 °C computed from Eq. 12. In addition, we provide one datum based on pyroxene-magnetite pair from the gabbro intrusion. Assuming that the minerals record original igneous values, the $\delta'^{18}O_{pyroxene}$ – $\delta'^{18}O_{magnetite}$ fractionation gives 2.6 ‰, which corresponds to equilibrium temperature of 890 °C (calibration from Valley et al., 2003).

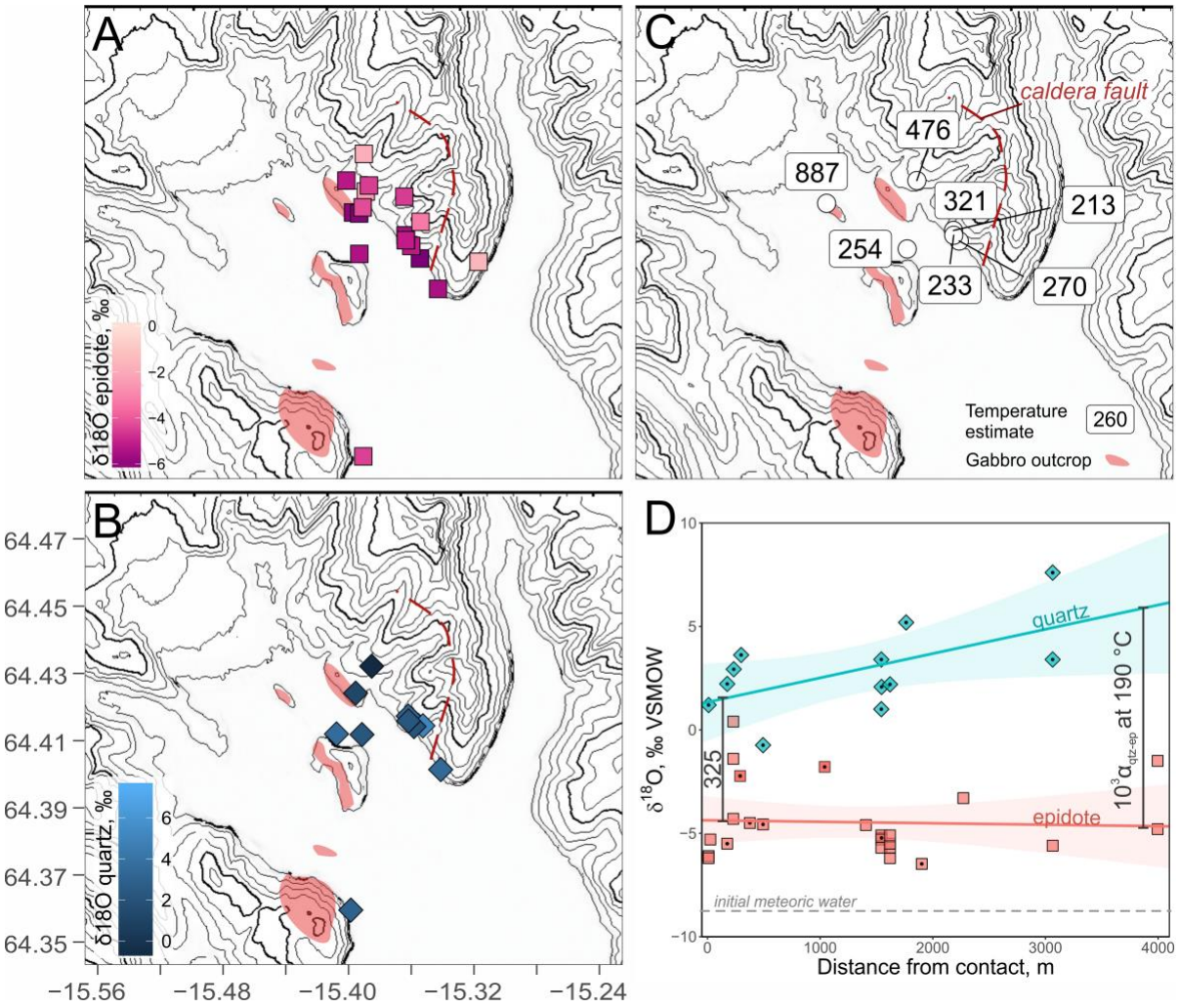

Figure 8. Spatial distribution of $\delta'^{18}O$ values in epidote (A) and quartz (B) from the host rocks of the Geitafell intrusion shown in the map view (see lithological legend in Fig. 1). The equilibrium temperatures computed from mineral pair measurements extracted from the same sample are shown in (C). The $\delta'^{18}O$ values plotted as a function of distance from the intrusion contact shown in panel (D). Based on the $\delta'^{18}O_{quartz\text{-}epidote}$ fractionation, the temperature around the intrusion is >325 °C near the contact and 190 °C away from it. The data is compiled from Pope et al., 2014 and this study (dotted symbols in D). The isotope equilibrium is consistent with the mineralogical pattern of alteration (Fridliefsson, 1983) and the fluid inclusion data (Troyer et al., 2007).

4. DISCUSSION

Our measurements of minerals and fluids are quite consistent with their respective fluid sources, confirming that $\Delta'^{17}O$ measurements provide useful constraints for tracking water-rock

interaction. These results validate previous studies of ancient submarine and continental hydrothermal systems that focused on the paleoenvironmental conditions of the early Paleoproterozoic (e.g. Herwartz et al., 2015; Zakharov et al., 2017; Zakharov and Bindeman, 2019; Zakharov et al., 2019). In these works, $\Delta'^{17}O$ values were measured to derive $\delta^{18}O$ of seawater or to evaluate mean annual temperature using estimated $\delta^{18}O$ values of local precipitation (Dansgaard, 1964). Below we consider how triple oxygen isotope measurements can be used to constrain the nature of combined isotope shifts owing to boiling, and isotope exchange, and temperature of mineral alteration based on calibrated thermometers. In addition, we explore the processes of crustal assimilation of hydrothermally altered rocks by mantle-derived magmas using the triple oxygen isotope coordinates.

4.1. Triple oxygen isotope shifts in fluids

The distinctly different slopes in the triple oxygen isotope space (see Fig. 3) allow us to interpret the origin of fluids in a new dimension. We use $\Delta'^{17}O$ directly measured in well fluids to capture possible isotope shifts occurring in modern hydrothermal systems that enable us to establish a basis for interpreting the mineral data and for understanding fossilized systems.

In the seawater-dominated Reykjanes system, the $\delta'^{18}O$ of well fluids are close to those of seawater with $\Delta'^{17}O$ around -0.02 ‰ (Fig. 4). Their $\delta'^{18}O$ values range between -0.2 and +1.1 ‰, not quite as high as in seawater-derived fluids measured at submarine vents (+0.5-2 ‰; Shanks, 2001). Together with the low δD values (-20 ‰), the isotope compositions of Reykjanes fluids hint at participation of meteoric water in the measured fluids (Arnórsson, 1978; Pope et al., 2011). The combined hydrogen and triple oxygen isotope values of these fluids reflect a combination of exchange with rocks at high temperature and up to 30 wt. % involvement of local meteoric water (see Fig. 6). The $\Delta'^{17}O$ values slightly below 0 ‰, are interpreted as the effect of

isotope exchange with rocks at high temperature reflecting the water-to-rock mass ratios (W/R) between 0.1 and 1 (Fig. 4). Finally, some contribution of steam to the well fluids is manifested by the δD values that are shifted negatively from the trajectories of exchange with MORB (Fig. 4 and 6).

Boiling that occurs in shallow hydrothermal systems should follow a slope similar to meteoric water line in the $\delta'^{18}O - \Delta'^{17}O$ space due equilibrium fractionation between vapor and liquid ($\theta_{vapor\text{-}liquid} = 0.529$; see Eq. 4). This value was constrained from low temperature experiments (< 50 °C; Barkan and Luz, 2005) and is likely higher, closer to 0.53, for boiling water at depth. Thus, boiling affects $\delta'^{18}O$ and δD values of fluids in accordance with liquid-vapor equilibrium fractionation (Horita and Weselowski, 1994), causing only small variations in $\Delta'^{17}O$. The well fluids at Krafla are derived from local meteoric waters ($\delta'^{18}O$ = - 13 ‰) and are enriched in heavy isotopes of oxygen so that their values approach -8 ‰ due to boiling and steam separation that occurs near the surface (Pope et al., 2016). At a temperature close to 100 °C, and the values of oxygen isotope fractionation, $\theta_{liquid\text{-}vapor} = 0.529$ (Barkan and Luz, 2005) and $1000\ln^{18/16}\alpha$ close to 5 ‰ (Horita and Weselowski, 1994), the $\delta^{18}O$ of remaining liquid can be computed as $R_{liquid} = R_{bulk} \cdot (1\text{-}f_{\alpha}) \cdot (1\text{-}f)^{\text{-}1}$. The measured values ($\delta'^{18}O$ between -8 and -6 ‰) correspond to about 70-90 % of remaining liquid fraction (value *f*) of the fluid that originally had $\delta'^{18}O$ of around -10 ‰ due to isotope exchange with rocks. Essentially, boiling and liquid-vapor separation would result in the $\Delta'^{17}O$ shifts of only about 0.005 ‰ (Fig. 5). The $\Delta'^{17}O$ values of these fluids are however shifted negatively by 0.01 ‰ with respect to the meteoric water line (Fig. 6), which we interpret to result from isotope exchange with rocks, as supported by previous measurements of unseparated geothermal fluids at Krafla (Ármannsson et al., 2014; Pope et al., 2016). The δD values actually clarify the effect of water-rock isotope exchange

combined with shallow boiling and steam loss that occurred between 100 and 200 °C (see Fig. 6). Consistent with the δD values of measured fluids and their triple oxygen isotope values, the isotope shifts measured in Krafla well fluids correspond to W/R ratio of about 1-2. We thus conclude, that the $\Delta'^{17}O$ values of Krafla fluid samples are less affected by the isotope exchange than the Reykjanes fluids, however carry a strong signature of boiling.

In all three systems we measured $\Delta'^{17}O$ shifts that range between -0.01 and -0.02 ‰ and about +0.5 to +2 ‰ shifts in $\delta'^{18}O$. Thus, water-rock interaction produces hydrothermal fluids that evolve along the slope of 0.510-0.516 in $\delta'^{17}O$-$\delta'^{18}O$ space, with the mean value of 0.512 for submarine systems (see Fig. 4B). Our estimate is based on the measurements of epidote and quartz extracted from modern ocean floor, where fluids appear to be shifted the most. This is similar to the previous estimate of 0.5105 provided by the study of bulk rock samples of altered oceanic crust (Sengupta and Pack, 2018). The value of this slope represents the input of high-temperature water-rock interaction in the triple oxygen isotope budget of hydrosphere, and it is an important variable because it allows to assess the slope and extent of other fluxes (see Sengupta and Pack, 2018).

4.2. Mineral record of $\Delta'^{17}O$ in fluids in the crust

At Reykjanes and Krafla, the measured $\Delta'^{17}O$ values of minerals are reflective of equilibrium fluids that were present at depth in the recent past, which for the most part are similar to the modern-day well fluids (Sveinbjornsdottir et al., 1986). Supporting this are epidotes that have $\Delta'^{17}O$ and $\delta'^{18}O$ values close to the modern-day sources of fluids owing to small equilibrium fractionation at high temperature ($10^3 \ln {}^{18/16}\alpha_{\text{epidote-water}} \approx$ 0-1 ‰; Zheng, 1993). Epidotes from Krafla and Geitafell, fall within the range of meteoric water values, while at Reykjanes, epidote compositions are very similar to seawater (Figs. 4 and 5). Also, one sample of garnet from the

576 Geitafell system has triple oxygen isotope composition close to that of meteoric water. It is
577 expected, that the $\Delta'^{17}O$ of minerals with small fractionation would be close to that of fluids, i.e.
578 within about 0.01 ‰ at these temperatures (Hayles et al., 2018). This small range, ±0.01‰, is at
579 the limit of analytical precision, thus precluding meaningful determination of the reason for
580 small variations in the $\Delta'^{17}O$ of epidotes. Nevertheless, epidotes provide promising first-order
581 estimates of $\Delta'^{17}O$ in equilibrium fluids and they reveal reaction with rocks in instances where
582 the fluids were shifted, as were epidotes recovered from modern oceanic crust (Fig. 4).
583 Using the calibrated quartz-water fractionation (Eq. 9 and 10; Sharp et al., 2016; Wostbrock
584 et al., 2018), we find that the $\delta'^{18}O$ values of computed equilibrium fluids at Reykjanes are lower
585 by about 1 ‰ than the directly measured modern-day well fluids and epidotes, while the $\Delta'^{17}O$
586 values are close to that of seawater-derived fluids (Fig. 4). Involvement of ancient (Pleistocene)
587 meteoric or glacial water (Sveinbjornsdottir et al., 1986; Pope et al., 2014) with low $\delta^{18}O$ values
588 would explain these values, as suggested by the low δD values of epodotes (Fig. 6). That
589 suggests that the $\delta'^{18}O$ values of epidotes are within 1 ‰ of their equilibrium fluids. Equilibrium
590 fluids computed from quartz-water fractionation at Krafla and Geitafell plot within the 95 %
591 prediction intervals around the meteoric water line which agrees well with the estimated values
592 of local fluid sources and with the epidote values (Fig. 5). The negative shifts in the $\Delta'^{17}O$ of
593 equilibrium fluids compared to meteoric water likely resulted from isotope exchange with rocks
594 at high temperature, while negative $\delta'^{18}O$ shifts could be a result of combined effects of isotope
595 exchange and liquid-steam separation with a high input of steam (see Fig. 5).
596 As an example of ancient hydrothermal alteration, the epidote and quartz $\delta'^{18}O$-$\Delta'^{17}O$
597 measurements from the 6 Ma Geitafell system indicate that the $\delta'^{18}O$ values of equilibrium fluids
598 range between −9 and −3 ‰, resembling previous estimates that were based on δD-$\delta^{18}O$ values

of epidotes (Pope et al., 2014). The $\Delta'^{17}O$ values of the Geitafell epidote (+0.01 to +0.03 ‰) are consistent with than of inferred meteoric water with $\delta'^{18}O$ of -8 ± 1 ‰, they plot directly on the meteoric water line (Fig. 5). This value is generally corroborated by the equilibrium fluids computed from quartz, however those are lower in $\Delta'^{17}O$ that epidote values and a bit more scattered. The value of -8 ‰ is somewhat high for precipitation in the interior of Iceland, where Geitafell was originally formed at 6 Ma (Fig. 1; Friðleifsson, 1983). In comparison, precipitation at the Krafla system located in the interior of the island has $\delta^{18}O$ of around -13 ‰. It is possible to interpret some of the reconstructed fluids as a result of meteoric water with $\delta'^{18}O$ lower than -8 ‰ combined with isotope exchange (see Fig. 5D). However, the δD values of epidotes and reconstructed equilibrium fluids (Pope et al., 2014) indicate meteoric water source with the $\delta^{18}O$ value of -8 ± 1 ‰ corroborating our $\Delta'^{17}O$ estimates (see Fig. 3 and Fig. 6).

We notice that the $\Delta'^{17}O$ values of equilibrium fluids derived from quartz measurements are consistently lower than that of epidote. This could be partially explained by the wide range of temperatures and isotope shifts recorded by quartz. The mineral forms over a large span of temperatures including late-stage veins at low temperature, as low as 150 °C. Thus, we realize that the applied mineral-water calibration might yield inaccurate equilibrium fluids due to due to inaccurate choice of equilibrium temperature and due to heterogeneities of oxygen isotope composition within quartz crystals as revealed by SIMS (Fig. 7). This particular crystal (Fig. 7A) was extracted from a relatively shallow depth of 744 meters, where borehole temperature measurements indicate a thermocline in which temperatures are consistently lower than the boiling point of water (Sveinbjornsdottir et al., 1986). In this case equilibrium temperature of 200 °C is likely a more accurate estimate (Fig. 7). The 4 ‰ variation measured within the crystal may related to a change in temperature or/and transition from rock- to meteoric-water-dominated

622 fluid isotope composition. The spatial distribution of $\delta^{18}O$ values in the rocks surrounding the
623 Geitafell intrusion display a pattern also consistent with non-isothermal equilibrium fractionation
624 of oxygen isotope ratios between quartz and water around plutons (Fig. 8) that were emplaced in
625 the shallow crust causing circulation of meteoric waters around them (see Taylor, 1974; Forester
626 and Taylor, 1979). The $\delta^{18}O$ values of epidote meanwhile vary much less than those of quartz,
627 partly due to its smaller fractionation factor and partly, due to high and a narrow range
628 temperatures recorded by the mineral (rarely above or below 250-400 °C; Bird and Spieler,
629 2004). Additionally, epidote is typically found in areas of high permeability within
630 hydrothermally altered matrix, where water/rock ratios are high (Bird and Spieler, 2004). We
631 thus suggest that $\Delta'^{17}O$ values of epidote (and garnet) can be used as a direct proxy for $\Delta'^{17}O$
632 values of equilibrium fluids, while caution is needed when using quartz-water calculations to
633 reconstruct equilibrium fluids.

634 ***4.5 Implications for magmatic assimilation and origin of low $\delta^{18}O$ rhyolites***

635 In areas of extensive magmatism shallow hydrothermally altered rocks can be assimilated by
636 partial melts to yield low- $\delta^{18}O$ igneous rocks. Similarly to radiogenic isotopes, major elements,
637 and trace elements, triple oxygen isotope composition of contaminated magmas can trace the
638 input of hydrothermally altered rock. In Krafla, erupted rhyolites, such as glasses quenched by
639 drilling of hole IDDP-1 and high silica rocks exposed on the surface carry a low-$\delta^{18}O$ signature
640 from assimilated hydrothermally altered crust (Elders et al., 2011). We construct the trajectory of
641 assimilation of shallow hydrothermally altered rocks in triple oxygen isotope space (Fig. 9)
642 based on our measurements of epidote and quartz, rhyolitic glasses and the previous
643 measurements of altered basalts by Herwartz et al. (2015) recalibrated to more accurate standards
644 (Pack et al., 2016). These measurements provide the basic information needed to estimate the

effect of crustal assimilation on the triple oxygen isotope composition of contaminated magmas. Since magmatic differentiation occurs at high temperature, the $\Delta'^{17}O$ values of primitive and evolved magmas do not vary significantly at the level of analytical precision in the range of values $\Delta'^{17}O$ = -0.06±0.01 ‰ (Tanaka and Nakamura, 2013; Pack and Herwartz, 2014; Pack et al., 2016; Sharp et al., 2018). Thus, incorporation of hydrothermally altered rocks with distinct isotope composition ($\Delta'^{17}O$ = +0.02 ± 0.01 ‰), could be resolved within the analytical precision. We estimate that the low-$\delta^{18}O$ rhyolitic magmas from Krafla, including those quenched and extracted by drill hole IDDP-1, were derived from assimilation of 10-20 % hydrothermally altered crust and 80-90 % uncontaminated magmas (Fig. 9). These estimates agree well with previous calculations based on combined oxygen and hydrogen isotope composition of the quenched glasses yielding about 20 % material assimilated (Elders et al., 2011). This approach for estimating the amount of assimilant through isotope mass balance might help to resolve the nature of recycled material in other geological situations where the contaminant has very high $\delta^{18}O$ and low $\Delta'^{17}O$ values, such as low temperature sedimentary rocks (e.g. shales with $\Delta'^{17}O$ = -0.10 ± 0.01 ‰; Bindeman et al., 2018).

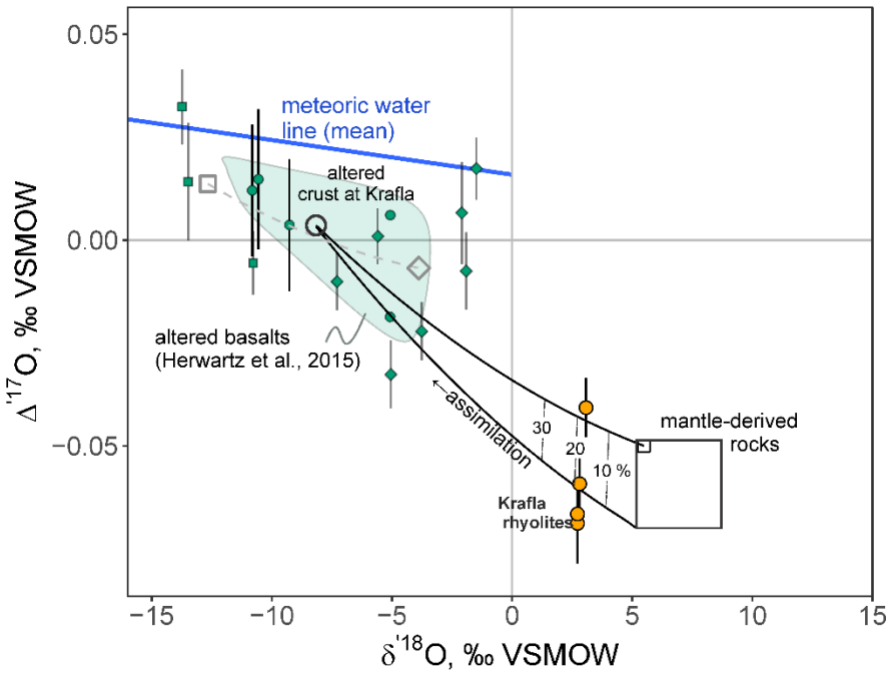

660

661 **Figure 9.** Triple oxygen isotope systematics of assimilation of low $\delta_{18}O$ hydrothermally altered crust at
662 Krafla by mantle-derived magmas. The contribution of low $\delta'_{18}O$ and high $\Delta'_{17}O$ hydrothermally altered
663 crust from Krafla is resolved due to its distinct isotope signature compared to the isotope composition of
664 uncontaminated magmas. Measurements of volcanic glasses quenched by the drilling hole IDDP-1 and
665 surface rhyolites are consistent with assimilation of 20 % of hydrothermally altered crust by mantle-
666 derived melts. The composition of hydrothermally altered crust is represented by average composition of
667 bulk hydrothermally altered basalts measured previously (data from Herwartz et al., 2015 recalibrated to
668 SCO composition from Pack et al., 2016) that can be also reproduced by mixing between average values
669 of epidote and quartz shown with open square and open diamond symbols, respectively.
670

671 **5. CONCLUSIONS**

672 We have presented high-precision measurements of $\Delta'_{17}O$ in hydrothermal minerals and
673 fluids from Icelandic geothermal areas Krafla and Reykjanes and from the fossilized
674 hydrothermal system at Geitafell. The measurements provide a record of isotope exchange
675 between rocks and variable fluid sources, such as seawater and meteoric waters of different
676 isotope composition. We found that:

1. Similar to combined δD and $\delta_{18}O$ measurements of hydrous minerals, the triple oxygen isotope measurements can fingerprint initial fluids, constrain temperature of alteration and effective water-rock ratios. Our results support previous triple oxygen isotope studies of the early Paleoproterozoic rocks that recorded composition of ancient precipitation (Herwartz et al., 2015; Zakharov et al., 2019) and seawater (Zakharov and Bindeman, 2019).
2. Measurements of high-temperature minerals, such as epidotes and garnet, provide a close estimate of $\Delta'_{17}O$ in the equilibrium fluids. In our case, epidote has isotope compositions almost identical to the local fluid sources at Reykjanes and Krafla. Geitafell epidotes record isotope composition of 6 Ma meteoric water with $\delta'_{18}O$ of -8 ± 1 ‰.
3. The $\Delta'_{17}O$ measurements of geothermal fluids collected at the surface present a novel way to resolve the effects of isotope exchange with rocks at high temperature and boiling, which complements the conventional δD-$\delta_{18}O$ measurements. The negative $\Delta'_{17}O$ shifts in fluids are due to high-temperature exchange between rocks and local fluid sources, whereas shifts in $\delta'_{18}O$ without a significant change in $\Delta'_{17}O$ are due to boiling and vapor-liquid separation.
4. Quartz are used here to derive equilibrium fluid values via calibrated equilibrium fractionation. The estimated fluids range within ±1.5 ‰ and ± 0.02 ‰ in $\delta'_{18}O$ and $\Delta'_{17}O$ of the well fluids at respective localities. However, caution is needed when interpreting the derived equilibrium fluid values due to presence of multiple generations of equilibrium compositions within single crystals as shown here with the *in situ* $\delta_{18}O$ measurements.
5. The $\delta'_{18}O$- $\Delta'_{17}O$ values of contaminated magmas might be used to inform about the amount of assimilated material. The measurements of low $\delta_{18}O$ rhyolites from Krafla are consistent with assimilation of 10-20 % of high-temperature hydrothermally altered crust.

ACKNOWLEDGEMENTS

700 We are grateful to the handling editor Karen Johannesson, Daniel Herwartz, Zachary Sharp, and
701 one anonymous reviewer for their careful reviews, comments and suggestions that greatly
702 improved the quality of the manuscript. We are thankful to Annette Mortensen from
703 Landsvirkjun Power Company, Finnbogi Óskarsson and Júlíana Signý Gunnarsdóttir from ISOR
704 for providing access to well fluids and mineral drill cuttings. We also thank Kouki Kitajima and
705 John Valley for conducting in situ $\delta_{18}O$ measurements of the quartz crystal (KJ36 744) *in situ* by
706 SIMS in the WiscSIMS Lab, University of Wisconsin. The WiscSIMS is supported by NSF grant
707 EAR-1658823. The manuscript was improved by discussions with Mike Hudak and Ryan
708 Seward. The funding is provided by National Geographic Society grant (CP-079ER-17),
709 Geological Society of America Graduate Research grant and Evolving Earth Foundation award
710 to DZ, NSF grants EAR-1447337 and 1833420 to IB and NSF grant EAR-0507181 to MR.

Table 1. Hydrogen and triple oxygen isotope measurements of minerals and fluids from Reykjanes, Krafla and Geitafell systems									
Drill hole/sample	Depth, m	Material	$\delta'^{18}O$	SE	$\Delta'^{17}O$ (λ_{RF}=0.528)	SE	δD	SE	H_2O, wt. %
Reykjanes									
RN12	1070	epidote	0.932	0.002	0.008	0.006			
RN12	1070	epidote	1.676	0.004	-0.023	0.007			
RN12	1070	quartz	5.582	0.004	-0.023	0.010			
RN12	1070	quartz	5.793	0.004	-0.029	0.013			
RN17B	2645	epidote	0.760	0.003	-0.032	0.006	-64.5	4	2.0
RN17B	2645	epidote	0.342	0.004	-0.013	0.010			
RN17B	2320	epidote	0.706	0.003	-0.021	0.007			
RN10		well fluids	1.141	0.001	-0.025	0.002	-21.7	1.9	
RN12		well fluids	-0.200	0.001	-0.017	0.002	-20.9	1.6	
RN12		well fluids	-0.125	0.001	-0.015	0.002	-20.9	1.6	
RN25		well fluids	0.818	0.001	-0.015	0.002	-22.4	2.1	
Krafla									
K06	1730	epidote	-13.482	0.006	0.014	0.014			
K06	1868	epidote	-13.732	0.003	0.033	0.009			
K36	744	quartz	-2.091	0.012	0.007	0.012			
K36	744	quartz	-1.482	0.008	0.017	0.008			
K36	744	quartz	-1.910	0.009	-0.008	0.009			
IDDP-1	1220	quartz	-5.048	0.004	-0.033	0.008			
IDDP-1	1220	quartz	-3.759	0.003	-0.022	0.007			
IDDP-1	1220	epidote	-10.777	0.003	-0.006	0.008			
K26	1020	quartz	-7.281	0.004	-0.010	0.007			
K21	550	quartz	-5.591	0.004	0.001	0.007			
IDDP-1	2095	rhyolitic glass	2.726	0.005	-0.069	0.010			

Table 1 *Continued*									
IDDP-1	2095	rhyolitic glass	2.724	0.008	-0.066	0.009			
IDDP-1	2095	rhyolitic glass	3.080	0.007	-0.040	0.007			
KRF14		rhyolitic glass	2.813	0.007	-0.059	0.007			
IDDP-01		well fluids	-7.903	0.001	0.007	0.002	-76.4	2.0	
KJ36		well fluids	-8.507	0.001	0.014	0.002	-80.4	2.0	
Klafla pool		powerplant discharge	-5.898	0.001	0.008	0.002	-76.6	2.1	
Geitafell									
GER 5		epidote	-5.234	0.005	0.005	0.011	-87.9	4	2.5
GER 5		quartz	2.073	0.003	-0.021	0.007			
GER1		garnet	-5.737	0.004	0.029	0.010			
GTF 25		epidote	-5.517	0.004	0.030	0.010	-95.9	4	2.3
GTF 25		quartz	2.219	0.004	0.002	0.009			
GTF28		epidote	-6.500	0.004	0.019	0.009	-72.5	4	1.7
GER16		quartz	-2.284	0.003	-0.003	0.008			
GER16		quartz	-1.011	0.004	-0.013	0.008			
GER34		quartz	1.978	0.004	-0.014	0.007			
GER34		quartz	1.451	0.003	0.019	0.007			

711

712 **REFERENCES**

713 Alt, J. C., & Teagle, D. A. H. (2000). Hydrothermal alteration and fluid fluxes in ophiolites and
714 oceanic crust. *Geological Society of America, Special Paper*, *349*, 273–282.

715 Árnason, B. (1976). Groundwater System in Iceland, Traced by Deuterium. *Societas*
716 *Scientiarum Islandica*, Reykjavik, 236.

717 Ármannsson, H., Fridriksson, T., Gudfinnsson, G. H., Ólafsson, M., Óskarsson, F., &
718 Thorbjörnsson, D. (2014). IDDP—The chemistry of the IDDP-01 well fluids in relation
719 to the geochemistry of the Krafla geothermal system. *Geothermics*, *49*, 66-75.

720 Arnórsson, S. (1978). Major Element Chemistry of the Geothermal Sea-Water at Reykjanes
721 and Svartsengi, Iceland. *Mineralogical Magazine*, *42*(322), 209–220.

722 Bao, H., Cao, X., & Hayles, J. A. (2016). Triple oxygen isotopes: fundamental relationships
723 and applications. *Annual Review of Earth and Planetary Sciences*, *44*, 463-492.

724 Barkan E. and Luz B. (2005) High precision measurements of 17O/16O and 18O/16O ratios in
725 H2O. *Rapid Commun. Mass Spectrom.* **19**, 3737–3742.

726 Bindeman I. N., Zakharov D. O., Palandri J., Greber N. D., Dauphas N., Retallack G. J.,
727 Hofmann A., Lackey J. S. and Bekker A. (2018) Rapid emergence of subaerial
728 landmasses and onset of a modern hydrologic cycle 2.5 billion years ago. *Nature* **557**,
729 545–548.

730 Bird, D. K., & Spieler, A. R. (2004). Epidote in Geothermal Systems. *Reviews in Mineralogy*
731 *and Geochemistry*, *56*(1), 235–300. https://doi.org/10.2138/gsrmg.56.1.235

732 Cao X. and Liu Y. (2011) Equilibrium mass-dependent fractionation relationships for triple
733 oxygen isotopes. *Geochim. Cosmochim. Acta* **75**, 7435–7445. Available at:
734 http://dx.doi.org/10.1016/j.gca.2011.09.048.

735 Craig, H. (1961). Isotopic variations in meteoric waters. *Science*, *133*(3465), 1702-1703.
736 Criss, R. E., & Taylor Jr, H. P. (1986). Meteoric-hydrothermal systems. *Reviews in*
737 *Mineralogy*, *16*, 373-424.
738 Dansgaard, W. (1964). Stable isotopes in precipitation. *Tellus* **16**, 436-468.
739 Darling, W. G., & Ármannsson, H. (1989). Stable isotopic aspects of fluid flow in the Krafla,
740 Námafjall and Theistareykir geothermal systems of northeast Iceland. *Chemical*
741 *Geology*, *76*(3-4), 197-213.
742 Dilles, J. H., Solomon, G. C., Taylor, H. P., & Einaudi, M. T. (1992). Oxygen and hydrogen
743 isotope characteristics of hydrothermal alteration at the Ann-Mason porphyry copper
744 deposit, Yerington, Nevada. *Economic Geology*, *87*(1), 44-63.
745 Dixon, J.E., Bindeman, I.N., Kingsley, R.H., Simons, K.K., Le Roux, P.J., Hajewski, T.R.,
746 Swart, P., Langmuir, C.H., Ryan, J.G., Walowski, K.J. and Wada, I., 2017. Light stable
747 isotopic compositions of enriched mantle sources: resolving the dehydration
748 paradox. *Geochemistry, Geophysics, Geosystems* **18**, 3801-3839.
749 Eiler, J. M. (2001). Oxygen isotope variations of basaltic lavas and upper mantle
750 rocks. *Reviews in mineralogy and geochemistry*, *43*(1), 319-364.
751 Elders W. A., Friðleifsson G. Ó., Zierenberg R. A., Pope E. C., Mortensen A. K.,
752 Guðmundsson Á., Lowenstern J. B., Marks N. E., Owens L., Bird D. K., Reed M.,
753 Olsen N. J., and Schiffman P. (2011) Origin of low $\delta_{18}O$ rhyolite magma that intruded a
754 geothermal well being drilled in a central volcano in Iceland. Geology **39**, 231-234.
755 Friðleifsson, G. Ó. (1983) The geology and the alteration history of the Geitafell central
756 volcano, southeast Iceland. In: Doctoral Dissertation. Grant Institute of Geology,
757 University of Edinburgh, United Kingdom, 371.

Giggenbach, W. F. (1992). Isotopic shifts in waters from geothermal and volcanic systems along convergent plate boundaries and their origin. *Earth and Planetary Science Letters*, *113*, 495–510.

Graham, C. M. (1981). Experimental hydrogen isotope studies III: Diffusion of hydrogen in hydrous minerals, and stable isotope exchange in metamorphic rocks. *Contributions to Mineralogy and Petrology*, *76*(2), 216-228.

Gregory R. T. and Taylor H. P. (1981) An oxygen isotope profile in a section of Cretaceous oceanic crust, Samail Ophiolite, Oman: Evidence for δ18O buffering of the oceans by deep (>5 km) seawater-hydrothermal circulation at mid-ocean ridges. *J. Geophys. Res. Solid Earth* **86**, 2737–2755. Available at: http://dx.doi.org/10.1029/JB086iB04p02737.

Hattori K. and Muehlenbachs K. (1982) Oxygen Isotope Ratios of the Icelandic Crust. *J. Geophys. Res.* **87**, 6559–6565.

Hayba, D. O., & Ingebritsen, S. E. (1997). Multiphase groundwater flow near cooling plutons. *Journal of Geophysical Research B: Solid Earth*, *102*(6), 12235–12252. https://doi.org/10.1029/97JB00552

Hayles, J. A., Cao, X., & Bao, H. (2017). The statistical mechanical basis of the triple isotope fractionation relationship. *Geochemical Perspectives Letters*, **3**, 1-11.

Hayles J., Gao C., Cao X., Liu Y. and Bao H. (2018) Theoretical calibration of the triple oxygen isotope thermometer. *Geochim. Cosmochim. Acta* **235**, 237–245. Available at: https://doi.org/10.1016/j.gca.2018.05.032.

Herwartz D., Pack A., Krylov D., Xiao Y., Muehlenbachs K., Sengupta S. and Di Rocco T. (2015) Revealing the climate of snowball Earth from Δ17O systematics of hydrothermal

780 rocks. *Proc. Natl. Acad. Sci.* **112**, 5337–5341. Available at:
781 http://www.pnas.org/lookup/doi/10.1073/pnas.1422887112.
782 Horita J. and Wesolowski D. J. (1994) Liquid-vapor fractionation of oxygen and hydrogen
783 isotopes of water from the freezing to the critical temperature. *Geochim. Cosmochim.*
784 *Acta* **58**, 3425–3437.
785 Hudak, M. R., & Bindeman, I. N. (2018). Conditions of pinnacle formation and glass hydration
786 in cooling ignimbrite sheets from H and O isotope systematics at Crater Lake and the
787 Valley of Ten Thousand Smokes. *Earth and Planetary Science Letters*, **500**, 56-66.
788 Kita, N. T., Ushikubo, T., Fu, B., & Valley, J. W. (2009). High precision SIMS oxygen isotope
789 analysis and the effect of sample topography. *Chemical Geology*, **264**, 43-57.
790 Kyser, T. K., & Kerrich, R. (1991). Retrograde exchange of hydrogen isotopes between
791 hydrous minerals and water at low temperatures. *Geochemical Society, Special*
792 *Publication*, *3*(3), 409–422.
793 Kyser, T. K., & O'Neil, J. R. (1984). Hydrogen isotope systematics of submarine
794 basalts. *Geochimica et Cosmochimica Acta*, *48*(10), 2123-2133.
795 Landais, A., Barkan, E., & Luz, B. (2008). Record of $\delta^{18}O$ and ^{17}O-excess in ice from Vostok
796 Antarctica during the last 150,000 years. *Geophysical Research Letters*, 35(2).
797 Luz B. and Barkan E. (2010) Variations of 17O/16O and 18O/16O in meteoric waters.
798 *Geochim. Cosmochim. Acta* **74**, 6276–6286.
799 Manning, C. E., & Ingebritsen, S. E. (1999). Permeability of the continental crust: Implications
800 of geothermal data and metamorphic systems. *Reviews of Geophysics*, *37*(1), 127-150.

801 Matsuhisa Y., Goldsmith J. R. and Clayton R. N. (1978) Mechanisms of hydrothermal
802 crystallization of quartz at 250 °C and 15 kbar. *Geochim. Cosmochim. Acta* **42**, 173–
803 182.
804 Matthews A. (1994) Oxygen isotope geothermometers for metamorphic rocks. *J. Metamorph.*
805 *Geol.* **12**, 211–219.
806 Miller, M. F. (2002). Isotopic fractionation and the quantification of ^{17}O anomalies in the
807 oxygen three-isotope system: an appraisal and geochemical significance. *Geochimica et*
808 *Cosmochimica Acta*, *66*(11), 1881-1889.
809 Muehlenbachs K. and Clayton R. N. (1976) Oxygen isotope composition of the oceanic crust
810 and its bearing on seawater. *J. Geophys. Res.* **81**, 4365.
811 Norton, D. L. (1984). Theory of hydrothermal systems. *Annual Review of Earth and Planetary*
812 *Sciences*, *12*(1), 155-177.
813 Ohmoto, H., & Rye, R. (1974). Hydrogen and Oxygen Isotopic Compositions of Fluid
814 Inclusions in the Kuroko Deposits , Japan. *Economic Geology*, *69*(November), 947–
815 953.
816 Ólafsson, J., & Riley, J. P. (1978). Geochemical studies on the thermal brine from Reykjanes
817 (Iceland). *Chemical Geology*, *21*(3-4), 219-237.
818 Pack A. and Herwartz D. (2014) The triple oxygen isotope composition of the Earth mantle and
819 understanding δO17 variations in terrestrial rocks and minerals. *Earth Planet. Sci. Lett.*
820 **390**, 138–145. Available at: http://dx.doi.org/10.1016/j.epsl.2014.01.017.
821 Pack A., Tanaka R., Hering M., Sengupta S., Peters S. and Nakamura E. (2016) The oxygen
822 isotope composition of San Carlos olivine on the VSMOW2-SLAP2 scale. *Rapid*
823 *Commun. Mass Spectrom.* **30**, 1495–1504.

824 Pope E. C., Bird D. K., Arnórsson S., Fridriksson T., Elders W. A. and Friðleifsson G. Ó.
825 (2009) Isotopic constraints on ice age fluids in active geothermal systems: Reykjanes,
826 Iceland. *Geochim. Cosmochim. Acta* **73**, 4468–4488.
827 Pope, E. C. (2011). *Hydrogen and oxygen isotope fractionation in hydrous minerals as*
828 *indicators of fluid source in modern and fossil metasomatic environments*. PhD thesis,
829 Stanford University.
830 Pope, E. C., Bird, D. K., & Arnórsson, S. (2014). Stable isotopes of hydrothermal minerals as
831 tracers for geothermal fluids in Iceland. *Geothermics*, *49*, 99–110.
832 https://doi.org/10.1016/j.geothermics.2013.05.005
833 Pope, E. C., Bird, D. K., Arnórsson, S., & Giroud, N. (2016). Hydrogeology of the Krafla
834 geothermal system, northeast Iceland. *Geofluids*, *16*(1), 175–197.
835 https://doi.org/10.1111/gfl.12142
836 Qi, H., Coplen, T.B., Gehre, M., Vennemann, T.W., Brand, W.A., Geilmann, H., Olack, G.,
837 Bindeman, I.N., Palandri, J., Huang, L. and Longstaffe, F.J., 2017. New biotite and
838 muscovite isotopic reference materials, USGS57 and USGS58, for δ2H measurements–
839 A replacement for NBS 30. *Chemical Geology*, **467**, 89-99.
840 Sharp Z. D., Gibbons J. A., Maltsev O., Atudorei V., Pack A., Sengupta S., Shock E. L. and
841 Knauth L. P. (2016) A calibration of the triple oxygen isotope fractionation in the SiO_2-
842 H_2O system and applications to natural samples. *Geochim. Cosmochim. Acta* **186**, 105–
843 119.
844 Sharp Z. D., Wostbrock J. A. G. and Pack A. (2018) Mass-dependent triple oxygen isotope
845 variations in terrestrial materials. *Geochemical Perspect. Lett.* **7**, 27–31.

Schoenemann, S. W., Schauer, A. J., & Steig, E. J. (2013). Measurement of SLAP2 and GISP $\delta^{17}O$ and proposed VSMOW-SLAP normalization for $\delta^{17}O$ and $^{17}O_{excess}$. Rapid Communications in Mass Spectrometry, 27(5), 582-590.

Sveinbjornsdottir A. E. (1991) Composition of geothermal minerals from saline and dilute fluids - Krafla and Reykjanes, Iceland. *Lithos* **27**, 301–315.

Sveinbjornsdottir A. E., Coleman M. L. and Yardley B. W. D. (1986) Origin and history of hydrothermal fluids of the Reykjanes and Krafla geothermal fields, Iceland - A stable isotope study. *Contrib. to Mineral. Petrol.* **94**, 99–109.

Tanaka and Nakamura (2013) Determination of ^{17}O-excess of terrestrial silicate/oxide minerals with respect to Vienna Standard Mean Ocean Water (VSMOW). *Rapid Commun. Mass Spectrom*, **27,** 285-297.

Taylor H. P. (1974) The Application of Oxygen and Hydrogen Isotope Studies to Problems of Hydrothermal Alteration and Ore Deposition. *Econ. Geol.* **69**, 843–883.

Taylor H. P. and Forester R. W. (1979) An oxygen and hydrogen isotope study of the Skaergaard Instrusion and its country rocks: A description of a 55-M.Y. old fossil hydorthermal system. *J. Pet.* **20**, 355–419.

Taylor H. P. (1971) Oxygen Isotope Evidence for Large-Scale Interaction between Meteoric Ground Waters and Tertiary Granodiorite Intrusions, Western Cascade Range, Oregon. *J. Geophys. Res.* **76**, 7855–7874.

Taylor, H. P. (1974). The Application of Oxygen and Hydrogen Isotope Studies to Problems of Hydrothermal Alteration and Ore Deposition. *Economic Geology*, *69*, 843–883.

Taylor, H. P. (1977). Water / rock interactions and the origin of in granitic batholiths. *Geological Society Special Publication, London*, *133*, 509–558.

869 Thorlacius, J. M. (1991). Petrological studies of the Geitafell central volcano, SE Iceland.
870 *MPhil Thesis. University of Edinburgh.*
871 Troyer R., Reed M.H., Elders W.A. and Friðleifsson G.O. Iceland Deep Drilling Project
872 (IDDP): Fluid Inclusion Microthermometry of the Geitafell Hydrothermal System. A
873 Possible Analog of the Active Krafla System? *AGU Fall meeting, San Francisco,*
874 *California, USA.*, v.V41A-03, 2007.
875 Truesdell, A. H., & Hulston, J. R. (1980). Isotopic evidence on environments of geothermal
876 systems. In *Handbook of environmental isotope geochemistry. Vol. 1*.
877 Uemura, R., Barkan, E., Abe, O., & Luz, B. (2010). Triple isotope composition of oxygen in
878 atmospheric water vapor. *Geophysical research letters*, **37**(4).
879 Urey, H. C. (1947). The thermodynamic properties of isotopic substances. *Journal of the*
880 *Chemical Society (Resumed)*, 562-581.
881 Valley, J. W., Bindeman, I. N., & Peck, W. H. (2003). Empirical calibration of oxygen isotope
882 fractionation in zircon. *Geochimica et Cosmochimica Acta*, *67*(17), 3257-3266.
883 Wostbrock J. A. G., Sharp Z. D., Sanchez-Yanez C., Reich M., van den Heuvel D. B. and
884 Benning L. G. (2018) Calibration and application of silica-water triple oxygen isotope
885 thermometry to geothermal systems in Iceland and Chile. *Geochim. Cosmochim. Acta*
886 **234**, 84–97. Available at: https://doi.org/10.1016/j.gca.2018.05.007.
887 Yeung, L. Y., Hayles, J. A., Hu, H., Ash, J. L., & Sun, T. (2018). Scale distortion from pressure
888 baselines as a source of inaccuracy in triple-isotope measurements. Rapid
889 Communications in Mass Spectrometry, 32(20), 1811-1821.

890 Zakharov D. O., Bindeman I. N., Slabunov A. I., Ovtcharova M., Coble M. A., Serebryakov N.
891 S. and Schaltegger U. (2017) Dating the Paleoproterozoic snowball Earth glaciations
892 using contemporaneous subglacial hydrothermal systems. *Geology* **45**, 667–670.
893 Zakharov, D. O., & Bindeman, I. N. (2019). Triple oxygen and hydrogen isotopic study of
894 hydrothermally altered rocks from the 2.43 – 2.41 Ga Vetreny belt , Russia : An insight
895 into the early Paleoproterozoic seawater. *Geochimica et Cosmochimica Acta*, *248*, 185–
896 209. https://doi.org/10.1016/j.gca.2019.01.014
897 Zakharov, D. O., Bindeman, I. N., Serebryakov, N. S., Prave, A. R., Azimov, P. Y., &
898 Babarina, I. I. (2019). Low $\delta_{18}O$ rocks in the Belomorian belt, NW Russia, and Scourie
899 dikes, NW Scotland: A record of ancient meteoric water captured by the early
900 Paleoproterozoic global mafic magmatism. *Precambrian Research*, 105431.
901 Zheng Y. F. (1993) Calculation of oxygen isotope fractionation in hydroxyl-bearing silicates.
902 *Earth Planet. Sci. Lett.* **120**, 247–263.